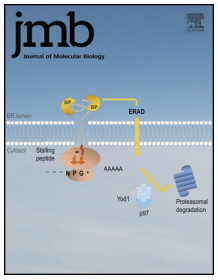

Clustering, Spatial Distribution, and Phosphorylation of Discoidin Domain Receptors 1 and 2 in Response to Soluble Collagen I

David A. Yeung [1], Nirvan Shanker [1], Anjum Sohail [2], Brent A. Weiss [1], Carolyn Wang [1], Jack Wellmerling [3], Subhadip Das [4], Ramesh K. Ganju [4], Jeanette L.C. Miller [5], Andrew B. Herr [5], Rafael Fridman [2] and Gunjan Agarwal [1,3]

*1 - **Biomedical Engineering Department,** the Ohio State University Columbus, OH 43210, USA*
*2 - **Department of Pathology and Oncology,** Wayne State University, Detroit, MI 48201, USA*
*3 - **Biophysics Program,** the Ohio State University, Columbus, OH 43210, USA*
*4 - **Department of Pathology,** the Ohio State University College of Medicine, Columbus, OH 43210, USA*
*5 - **Division of Immunobiology,** Cincinnati Children's Hospital Medical Center, Cincinnati, OH 45267, USA*

***Correspondence to Gunjan Agarwal:** 288 Bevis Hall, 1080 Carmack Road, Columbus, OH 43210, USA.*
agarwal.60@osu.edu
https://doi.org/10.1016/j.jmb.2018.11.015
Edited by Ichio Shimada

Abstract

Discoidin domain receptors (DDR1 and DDR2) are receptor tyrosine kinases that signal in response to collagen. We had previously shown that collagen binding leads to clustering of DDR1b, a process partly mediated by its extracellular domain (ECD). In this study, we investigated (i) the impact of the oligomeric state of DDR2 ECD on collagen binding and fibrillogenesis, (ii) the effect of collagen binding on DDR2 clustering, and (iii) the spatial distribution and phosphorylation status of DDR1b and DDR2 after collagen stimulation. Studies were conducted using purified recombinant DDR2 ECD proteins in monomeric, dimeric or oligomeric state, and MC3T3-E1 cells expressing full-length DDR2-GFP or DDR1b-YFP. We show that the oligomeric form of DDR2 ECD displayed enhanced binding to collagen and inhibition of fibrillogenesis. Using atomic force and fluorescence microscopy, we demonstrate that unlike DDR1b, DDR2 ECD and DDR2-GFP do not undergo collagen-induced receptor clustering. However, after prolonged collagen stimulation, both DDR1b-YFP and DDR2-GFP formed filamentous structures consistent with spatial re-distribution of DDRs in cells. Immunocytochemistry revealed that while DDR1b clusters co-localized with non-fibrillar collagen, DDR1b/DDR2 filamentous structures associated with collagen fibrils. Antibodies against a tyrosine phosphorylation site in the intracellular juxtamembrane region of DDR1b displayed positive signals in both DDR1b clusters and filamentous structures. However, only the filamentous structures of both DDR1b and DDR2 co-localized with antibodies directed against tyrosine phosphorylation sites within the receptor kinase domain. Our results uncover key differences and similarities in the clustering abilities and spatial distribution of DDR1b and DDR2 and their impact on receptor phosphorylation.

© 2018 Elsevier Ltd. All rights reserved.

Introduction

Discoidin domain receptors (DDR1 and DDR2) are widely expressed receptor tyrosine kinases that regulate a variety of cellular processes including cell adhesion, differentiation, proliferation and migration [1], collagen fibrillogenesis [2–4], and remodeling of the extracellular matrix [5]. Collagen(s) is the only known ligand for DDRs [6]. Both the collagen binding domains of the receptors [7–10] and their binding site on the collagen triple helix [11–14] have been elucidated in recent years. In addition, it has been established that DDRs exist as constitutive homodimers on the cell membrane prior to collagen binding and receptor activation [15–17]. DDRs undergo slow and sustained receptor activation upon ligand binding. However, the reasons for the delayed kinetics of DDR phosphorylation upon ligand binding remain poorly defined. Receptor clustering or higher order receptor oligomerization has been postulated by us [16,18] and others [17,19–21] as important modulators of both DDR–collagen interaction and receptor phosphorylation.

© 2018 Elsevier Ltd. All rights reserved.

Various domains of DDR1 have been shown to be important for receptor clustering and its oligomeric status. It is now understood that (i) dimerization [7] and higher-order oligomerization [12,18] of the DDR1 extracellular domain (ECD) enhance its binding to collagen; (ii) DDR1 exists as non-covalent homodimer on the cell surface, which is mediated by critical residues within its ECD [17] and transmembrane domain (TMD) [15]; (iii) both full-length and kinase-dead DDR1 expressed on the cell surface undergo clustering upon collagen binding [16–18,20,21]; and (iv) clustering of DDR1 post-ligand binding is mediated in part by its ECD [18] and by its intracellular domain (ICD) [20,21]. DDR1 clustering has been postulated to be a mechanism required for receptor activation based on our earlier microscopy-based studies [16,18], X-ray crystallographic insights by Carafoli *et al*. [10] and recent cell-based studies [20]. In this regard, mutation of an *N*-glycosylation site in the DDR1 ECD (which results in a higher population of dimers) has been shown to induce ligand-independent activation of DDR1 [17]. In another study, a function-blocking monoclonal antibody, which binds to DDR1 ECD and inhibits collagen-induced receptor phosphorylation [10], also inhibited DDR1 clustering [21]. Thus, understanding the structural constrains and molecular mechanisms that promote the clustering and/or the oligomeric state of DDR1 could be exploited as a therapeutic avenue to modulate receptor function in diseases involving DDR1 activity.

In contrast to DDR1, the role of oligomerization and/or clustering of DDR2 in mediating its interactions with collagen is less understood. Current data show that in DDR2, like in DDR1, (i) dimerization [7] and higher-order oligomerization of its ECD [11,22] enhance its binding to collagen, and (ii) in cells, DDR2 exists as a constitutive non-covalent homodimer [15], which is partly promoted by high propensity of the TMD of DDR2 to self-interact [23]. A juxtamembrane segment in the ICD of DDR2 has also been shown to control receptor dimerization and thereby regulate collagen-dependent activation [24]. However, studies on DDR2 clustering, spatial distribution and its correlation with receptor phosphorylation post-ligand binding are lacking.

To gain more insight into the role of the oligomeric state and clustering of DDR2 ECD in its interaction with collagen, we utilized ECD constructs of DDR2 capable of displaying monomeric, dimeric or oligomeric forms. These proteins were then used to test how these different oligomeric states of the ECD bind collagen and regulate fibrillogenesis of pepsin-digested and acid-soluble collagen I molecules. Atomic force microscopy (AFM) was used to follow the oligomeric state of monomeric and dimeric DDR2 ECD upon binding to collagen. Immunocytochemistry (ICC) coupled with fluorescence microscopy was used to evaluate collagen morphology, receptor clustering, spatial distribution and phosphorylation in cells expressing fluorescently-tagged full-length DDR2 or DDR1b. Our results demonstrate similarities and differences between DDR2 and DDR1b post-ligand binding with respect to receptor clustering and spatial distribution as well as how these processes influence DDR–collagen interactions and receptor phosphorylation.

Materials and Methods

Cell culture

MC3T3-E1 Subclone 4 cells were obtained from the American Type Culture Collection (ATCC, Rockville, MD) and cultured in minimum essential media (MEM)α supplemented with 2 mM L-glutamine, 1 mM sodium pyruvate and 10% fetal bovine serum. HEK293T and Cos1 cells were obtained from the ATCC and cultured in Dulbecco's modified Eagle medium (DMEM; Life Technologies Corporation, Grand Island, NY) supplemented with 10% fetal bovine serum (Life Technologies Corporation) and 1% Penicillin/Streptomycin.

Collagen and antibodies

Pepsin-digested bovine-dermal collagen (PureCol) and acid-extracted rat-tail collagen I were purchased from Advanced BioMatrix San Diego, CA, and Sigma Chemicals, St. Louis, MO, respectively. Mouse monoclonal (MAB25381) and goat polyclonal (AF2538) anti-DDR2 antibodies (raised against a peptide sequence in the DDR2 ECD) and rabbit monoclonal against phospho-DDR2 (DDR2-Y740, catalog no. MAB25382) were obtained from R&D Systems, Minneapolis, MN. Rabbit monoclonal antibodies recognizing phosphorylated DDR1b and DDR1c (DDR1b/c-Y513, catalog no. 14531), monoclonal antibody recognizing total DDR1 (D1G6, catalog no. 5583), polyclonal antibody recognizing phospho-DDR1 (DDR1-Y792, catalog no.11994), polyclonal antibody recognizing total DDR2 (catalog no.12133) and DyLight™ 554 Phalloidin (catalog no. 13054) were all purchased from Cell Signaling Technology, Danvers, MA. Anti-collagen I antibody (catalog no. 600-401-1035) was obtained from Rockland Immunochemicals, Limerick, PA. Antibodies to cortactin, vimentin and vinculin were from Bethyl Labs (Montgomery, TX), Cell Signaling and (R&D Systems), respectively. Mouse monoclonal antibodies, anti-Fc and anti-V5, were purchased from Jackson Immunoresearch (West Grove, PA) and Invitrogen (Carlsbad, CA), respectively. Monoclonal antibody recognizing β-actin was from Millipore Sigma. Anti-mouse, anti-rabbit and anti-goat IgG horseradish peroxidase-conjugated secondary antibodies were obtained from Santa Cruz Biotech and Thermo Scientific Pierce, Grand Island, NY. Anti-rabbit Alexa-Fluor568-conjugated secondary

antibody was purchased from Life Technologies (Carlsbad, CA).

DDR expression vectors

For expression of recombinant DDR2 ECDs, we used a DDR2-V5-His construct comprising the entire mouse DDR2 ECD tagged with a V5 epitope and 6His at the C-terminus as has been described earlier [2], and a DDR2-Fc, consisting of human DDR2 ECD harboring an IgG2 Fc fragment at the C-terminal end cloned into the pcDNA3.1/Myc-His expression vector as described for DDR1-Fc [17] (Fig. 1a). For expression of full-length DDRs in cells, we purchased an expression vector containing the human DDR2 cDNA tagged with green fluorescent protein (GFP) at the C-terminus from Origene (Rockville, MD). An expression vector encoding mouse DDR1b tagged with yellow fluorescent protein (YFP) was described previously [16].

Expression and purification of recombinant DDR2 ECD proteins

To obtain DDR2 ECDs displaying different oligomeric states, we used DDR2 ECD constructs in which the C-terminal region of the ECD was fused with either the Fc portion of the IgG molecule to generate DDR2-Fc or a V5-His tag to generate DDR2-V5-His (Fig. 1a). The Fc portion of the IgG molecule is known to undergo spontaneous dimerization and to generate oligomeric species in the presence of anti-Fc antibodies. Thus, the recombinant DDR2-Fc ECD fusion protein (DDR2-Fc) is expected to display a dimeric state, which can be induced to generate oligomeric forms upon incubation with the anti-Fc antibody. On the other hand, the recombinant DDR2-V5-His ECD protein is expected to display a monomeric form.

The recombinant proteins were expressed in human kidney HEK293T cells. Briefly, cells were seeded on collagen-coated 100-mm dishes. Cells grown to 75% confluence were transiently transfected with plasmids encoding either human DDR2-Fc or mouse DDR2-V5 cDNA, using *Trans*IT LT-1 transfection agent (Mirus Bio LLC), according to the manufacturer's protocol. Twenty-four hours after transfection, the cells were re-fed with fresh serum-free DMEM. The cells were then cultured in serum-free DMEM, and the conditioned media were collected and replaced with fresh serum-free DMEM, every 2–3 days for 7 to 10 days. The collected media were centrifuged (200*g*, 5 min) to remove cell debris and stored at 4 °C until use.

For purification of DDR2-V5-His protein, the harvested media were dialyzed overnight (12–14 kDa MWCO) at 4 °C in 20 mM Tris–HCl (pH 7.4) with 300 mM NaCl. Thereafter, the media were loaded into a 5-ml His-trap column (GE Healthcare Life Sciences) pre-equilibrated with 20 mM Tris–HCl (pH 7.4) and 300 mM NaCl. The column was then washed with equilibrium buffer, and the bound protein was eluted using a linear gradient of imidazole in a GE Amersham FPLC system. Fractions eluted between 120 and 150 mM imidazole were analyzed using SDS-PAGE followed by Coomasie Blue staining and/or Western blotting to detect purified DDR2-V5-His. Selected fractions were pooled and subjected to a buffer exchange using a Superdex200 gel filtration column equilibrated in TBS [20 mM Tris–HCl (pH 7.4), 150 mM NaCl].

DDR2-Fc was purified using a procedure very similar to that used for human DDR1b-Fc, as described [17]. Briefly, the harvested media were dialyzed in a solution of 25 mM NaH_2PO_4 (pH 7.5) and 150 mM NaCl for 24 h, and then loaded onto a 5-ml HiTrap Protein A Column (GE Healthcare Life Sciences) pre-equilibrated with 25 mM NaH_2PO_4 (pH 7.0) and 150 mM NaCl. The column was then

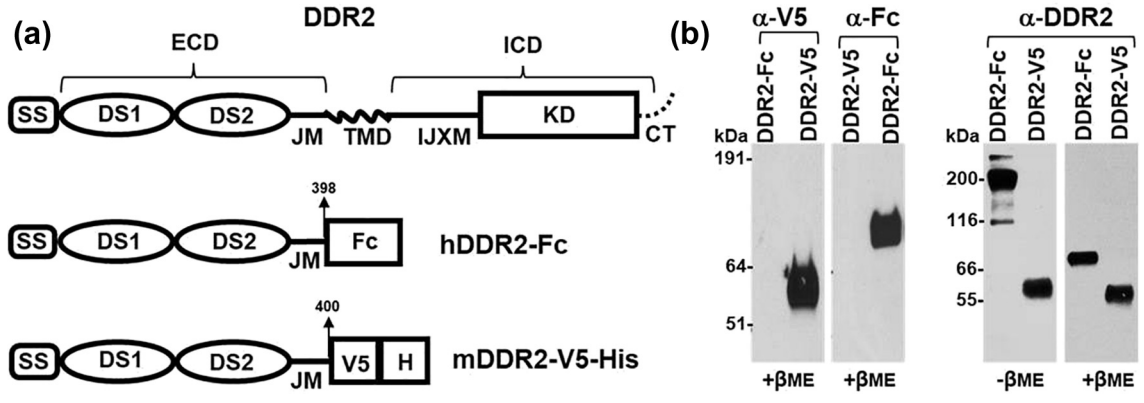

Fig. 1. (a) Schematic diagram showing the structure of full-length DDR2, human DDR2-Fc, and mouse DDR2-V5-His constructs. SS, signal sequence; DS, discoidin domain; ECD, extracellular domain; IJXM, intracellular juxtamembrane region; TMD, transmembrane domain; ICD, intracellular domain; KD, kinase domain. (b) Purified recombinant DDR2-V5-His and DDR2-Fc proteins (20 ng/lane) were resolved by SDS-PAGE under reducing conditions (+βME), either with 4%–12% (w/v) Bis–Tris gels (left panel) or under reducing and non-reducing (−βME, 100 ng/lane) conditions with 10% SDS-PAGE (right panel). The separated protein was detected by immunoblotting using anti-epitope or anti-DDR2 antibodies as indicated.

washed with 25 mM NaH_2PO_4 (pH 7.0) and 150 mM NaCl, and the bound protein was eluted using glycine buffer (pH 2.5). The eluate fractions (2 ml) were collected into tubes containing 200 µl of 1 M Tris (pH 8.0) and resolved by SDS-PAGE followed by Coomasie Blue staining and/or Western blotting. The fractions containing DDR2-Fc were pooled and dialyzed against phosphate-buffered saline (PBS) (pH 7.5) for 48 h at 4 °C.

Purified proteins were concentrated using an Amicon® Ultra Centrifugal Filter Device (Millipore) with a 10k MWCO, and the protein concentrations were determined using absorbance at 280 nm. The monomeric/dimeric state of the recombinant proteins was determined by SDS-PAGE under reducing and non-reducing conditions followed by Western blotting, using antibodies against the DDR2 ECD or the epitope tag (anti-Fc or anti V5), as previously described [22].

Solid-phase binding assays

A monomeric solution of bovine-dermal (or rat tail) collagen I in ice-cold PBS was immobilized in 96-well micro-titer plates by incubating the wells with 100 µl of 25 µg/ml of collagen, overnight at 4 °C. Thereafter, the plates were washed three times with 200 µl TBS (Tris-buffered saline) (Bio-Rad, Hercules, CA) containing 0.05% Tween 20 (GE Healthcare, Uppsala, Sweden), followed by blocking with 300 µl of 1% bovine serum albumin (Santa Cruz Biotechnology, Santa Cruz, CA) with 0.05% Tween overnight at 4 °C. The wells were washed again three times with TBS–tween and incubated with 100 µl of recombinant DDR2-V5-His or DDR2-Fc (before and after pre-oligomerization) at concentrations ranging from 0 to 20 µg/ml, overnight at 4 °C. To induce oligomerization of DDR2-Fc, the protein was incubated with an equal mass of anti-Fc antibody in PBS at 4 °C overnight, as previously described [22]. To detect binding of recombinant proteins to collagen, the plates were washed and thereafter probed with anti-DDR2 monoclonal antibodies (1:1000), followed by washing and incubating with horseradish peroxidase-conjugated secondary antibodies (1:2000). Bound protein was detected by adding 100 µl of 3,3′,5,5′-tetramethylbenzidine to each well for 20 min at room temperature with no light exposure. The reaction was stopped using 1 N HCl solution, and the absorbance was recorded at 450 nm using a spectrophotometer. All experiments were performed at least three times. The half maximal effective concentration (EC_{50}); that is, the concentration of DDR2 ECD protein required to yield a binding response halfway between the baseline and maximum was determined as described earlier [18]. Student's unpaired two-tailed *t* test was conducted on the EC_{50} values obtained for binding of dimeric or oligomeric DDR2 ECD to immobilized collagen from at least n = 3 experiments. A *p* value <0.05 was considered significant.

Collagen fibrillogenesis assay

Collagen fibrillogenesis was assessed by measuring the turbidity of neutralized collagen I solutions with a rise in temperature. To this end, 250 µl of ice-cold collagen solutions (200 µg/ml) in PBS (pH 7.5) containing 40 µg/ml of recombinant DDR2-V5-His or DDR2-Fc proteins (before and after pre-oligomerization) were incubated in 96-well Costar clear polystyrene plates at 37 °C. A collagen solution with or without anti-Fc antibody (40 µg/ml) was used as a control. The absorbance values were monitored every hour at 405 nm for up to 6 h using a spectrophotometer. Student's unpaired two-tailed *t* test was conducted on the absorbance values obtained at 6 h from at least n = 3 experiments. A *p*-value <0.05 was considered significant.

Atomic force microscopy

Monomeric collagen (1 µg/ml) was mixed with monomeric DDR2-V5-His or dimeric DDR2-Fc proteins (1 µg/ml in DDR2 concentration) in ice-cold PBS and incubated at 4 °C for 4 h. As a control, the recombinant DDR2 ECD proteins (without collagen) were also incubated in PBS under similar conditions. After 4 h of incubation, the samples were aliquoted onto chilled and freshly cleaved mica substrates, incubated for 5 min, washed and air dried and subjected to AFM imaging using the Multimode AFM (Digital Instruments, Santa Barbara, CA) as described earlier [18]. AFM imaging was performed in tapping mode in ambient air using NSC15 cantilevers (Micromasch, Estonia) with a nominal spring constant of 40 Nm^{-1}. Both height and amplitude images were recorded at 512 lines per scan direction. Topographic heights of DDR2 proteins and collagen filaments were measured from AFM images, by the section analysis feature of the Nanoscope software. At least n = 50 particles were analyzed using three identical replicates for each sample type (except for DDR2-V5-His bound to collagen for which n = 22 due to the low number of binding events). Student's unpaired two-tailed *t* test was used to determine statistically significant differences in height measurements across samples. A $p < 0.05$ was considered significant.

Transient transfection and Western blotting for receptor phosphorylation

MC3T3-E1 or Cos1 cells were split the day before transfection to 50%–60% confluence in 6-well or 60-mm tissue culture plates, respectively. The next day, DDR1b-YFP or DDR2-GFP plasmid DNA was transfected using TransIT®-LT1 Transfection Reagent (Mirus Bio LLC) according to the manufacturer's instructions. Forty-eight and 24 h post-transfection for MC3T3-E1 and Cos1 cells, respectively, the culture

medium was aspirated and the cells were washed twice with PBS before subjecting them to serum starvation in serum-free medium for 18 h. Then, the cells received 20 μg/ml (final concentration) of either rat-tail collagen I or vehicle (20 mM acetic acid) in serum-free media at 37 °C. At various time intervals, the cells were washed twice with cold PBS, and then lysed in RIPA buffer [50 mM Tris–HCl (pH 7.4), 150 mM NaCl, 1% NP-40, 0.25% sodium deoxycholate and 1 mM EDTA] supplemented with protease inhibitors (Protease Inhibitor Cocktail Set III, EDTA-Free; Millipore Sigma) and 10 mM NaF and 2 mM sodium orthovanadate. The cell lysates were cleared by centrifugation at 14,000*g* at 4 °C for 15 min, and the protein concentration was determined using the BCA kit (Thermo Scientific Pierce). Cell lysates were then frozen at −80 °C until used.

Unless otherwise stated, 25 μg of cell lysates was resolved by reducing 7.5% SDS-PAGE. Proteins were then transferred to a nitrocellulose membrane using conventional methods. The blots were probed with specific antibodies to DDRs or other proteins of interest. Membranes were incubated with corresponding IgG horseradish peroxidase-conjugated secondary antibodies and developed with ECL reagent (Thermo Scientific Pierce). Membranes were re-probed as stated in the figure legends after stripping with Western-Re-Probe reagent (Millipore Sigma). β-Actin was used for loading control.

Fluorescence microscopy of cells

MC3T3-E1 cells were cultured in complete MEMα media, as described above. Cells were seeded on glass bottom culture dishes (MatTek Glassware, Ashland, MA), for live cell imaging and on polylysine-coated coverslips for fixation and ICC. Transient transfection with DDR2-GFP or DDR1-YFP cDNA constructs was performed using *Trans*IT LT-1 transfection reagent (Mirus Bio LLC). As a control, a set of cells were non-transfected. Forty-eight hours after transfection, the cells were serum-starved for 12 to 18 h, and thereafter stimulated with bovine-dermal (or rat-tail) collagen I (20 μg/ml). For live cell imaging, the cells were imaged immediately before and after collagen stimulation at times indicated.

ICC was performed to evaluate receptor phosphorylation in MC3T3-E1 cells expressing DDR1-YFP or DDR2-GFP. At specific times (0, 30 min, and 4 h) after collagen stimulation, the cells were washed (two times in PBS) and then fixed in 4% paraformaldehyde (in PBS) for 10 min at room temperature. Thereafter, the cells were washed (three times in PBS) and permeabilized using 0.05% Triton X (in PBS with 2% BSA) for 10 min at room temperature. After subsequent washing, the cells were blocked with 2% BSA in PBST (PBS with 0.1% Tween) for 1 h at room temperature, and then incubated overnight with primary antibodies (1:500 for Y513, Y792, Y740, cortactin) and (1:200 for vinculin and vimentin) as indicated. Thereafter, the cells were washed, incubated with Alexa-Fluor568 conjugated secondary antibodies (1:3000 in PBST with 2% BSA in PBST) for 1 h at room temperature, and washed and mounted onto glass slides using the Duolink mounting media containing DAPI nuclear stain (from Sigma). ICC using collagen antibodies (1:500) was performed as detailed above but without the permeabilization step. For f-actin staining, after permeabilization and blocking, instead of the primary antibody step, the samples were incubated with Phalloidin (1:1000) for 30 min at room temperature and thereafter washed and mounted.

Images were acquired using on a Zeiss Axiovert (equipped with a Hamamatsu camera) [16] or a Zeiss Imager Z2 (equipped with an Axiocam ICc5 camera) light microscope with appropriate filter cubes for YFP, GFP, TRITC, and DAPI fluorescence. Wide-field fluorescence images were acquired using a 40× oil or a 63× water or oil-immersion objective lens. Fiji ImageJ was used to analyze the fluorescence microscopy images. To quantify small, asymmetrical punctuate structures (characteristic of DDR1b clusters), a threshold was applied to the images, after which all particles with an area less than 10 μm^2 and a circularity parameter <1 were counted (Fig. S1a; in ImageJ, the circularity parameter from 1 to 0 indicates departure from a perfect circle to an increasingly elongated shape). The number of punctuate structures per cell was thus determined for n = 8 cells for each sample type. The lengths of filamentous structures observed in DDR1b-YFP- and DDR2-GFP-expressing cells were ascertained by manually hand-tracing a segmented line to determine their maximum un-interrupted length (i.e., its contour length before a filament encounters a joint or a tangle, Fig. S1b). At least n = 85 filaments obtained from n = 12 cells were examined for each sample type. The Pearson's correlation coefficient (*R*) for co-localization of total DDR1b-YFP or DDR2-GFP with collagen or with phosphorylated (pDDR1 or pDDR2) receptor signal in ICC images was determined by using the Coloc2 plugin in Fiji ImageJ. Regions of interest (ROIs) were identified by tracking YFP/GFP-positive clusters or segments of filamentous structures by using the free-hand line tool. Student's unpaired two-tailed *t* test was used to determine statistically significant differences across *R* values obtained from at least n = 10 ROIs with (+) or without (–) a corresponding antibody (TRITC channel) signal. A $p < 0.05$ was considered significant.

Results

Using surface plasmon resonance, we previously demonstrated that oligomeric forms of DDR2-Fc displayed enhanced ability to bind bovine-dermal collagen I when compared to dimeric forms of DDR2-Fc [22]. In addition, in separate studies, we showed that monomeric DDR2-V5-His [2], dimeric DDR2-Fc

[25], and oligomeric DDR2-Fc [22] forms could all inhibit collagen I fibrillogenesis. However, in these earlier studies, the relative abilities of these structural states of the DDR2 ECD could not be compared side by side because of the different experimental conditions used. Here, under identical experimental conditions, we examined the relative abilities of the DDR2 ECD, in its various oligomeric states, to bind to soluble collagen I and modulate its fibrillogenesis. Studies were conducted using telopeptide-lacking bovine-dermal collagen as well as telopeptide-containing rat-tail collagen I.

The monomeric/oligomeric states of DDR2-V5-His and DDR2-Fc were confirmed by Western blotting under reducing and non-reducing conditions. As shown in Fig. 1b, DDR2-V5-His exhibited a relative molecular mass of ~60 kDa under both reducing and non-reducing conditions, consistent with this protein being in a monomeric state. In contrast, when resolved under non-reducing conditions, DDR2-Fc displayed a molecular mass of ~190 kDa, consistent with being an Fc-tagged dimer [22]. Under reducing conditions, DDR2-Fc displayed a mass of ~90 kDa. The oligomeric state of DDR2-Fc oligomers, induced by the presence of anti-Fc antibodies, was determined earlier using size-exclusion chromatography [22].

Effect of the oligomeric state of DDR2 ECD on collagen binding and fibrillogenesis

The ability of the recombinant DDR2 ECDs to bind to immobilized collagen I was evaluated using solid-phase binding assays. As shown in Fig. 2a, the binding of DDR2 ECD to the immobilized bovine-dermal collagen I was dependent on the oligomeric state of the ECD. The antibody induced-oligomeric DDR2-Fc displayed the highest binding followed by the dimeric DDR2-Fc and the monomeric DDR2-V5-His form. The anti-Fc antibody alone showed no binding to collagen I (data not shown). Quantitative analyses showed that, at equal DDR2 ECD concentrations, the EC50 for the oligomeric DDR2-Fc was (1.7 ± 1.5 μg/ml), about 4-fold lower than that of dimeric DDR2-Fc (6.8 ± 2.5 μg/ml; $p < 0.05$). The EC50 for DDR2-V5-His could not be determined due to the low levels of binding under the conditions tested. Similar results were obtained when experiments were conducted using rat-tail collagen I (Fig. S2a).

Collagen I fibrillogenesis can be induced *in vitro* by incubating monomeric chains of acid-solubilized collagen I in neutral pH at physiological temperature [22]. We therefore examined the extent of collagen I fibrillogenesis as a function of the oligomeric state of the DDR2 ECD proteins. As shown in Fig. 2b, a solution of neutralized bovine-dermal collagen I displayed a time-dependent increase in turbidity (absorbance) reaching a maximum after ~5 h (at

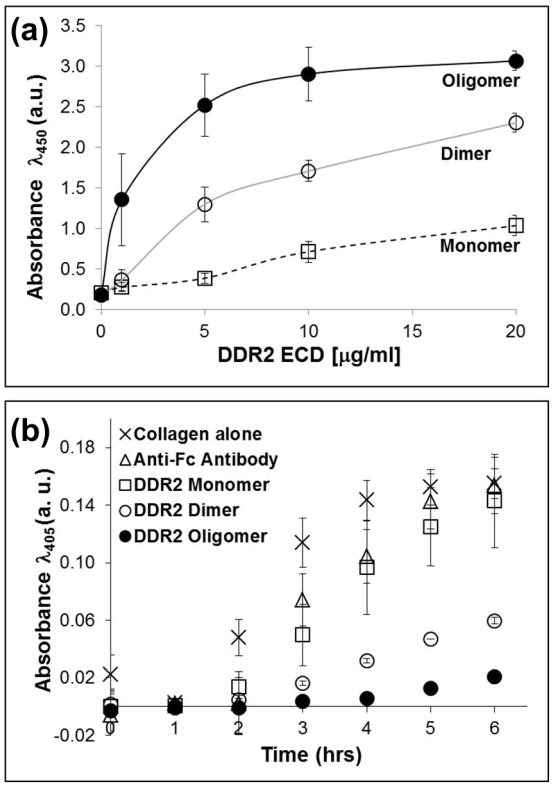

Fig. 2. (a) Solid-phase binding of DDR2 ECD proteins to immobilized bovine-dermal collagen I as indicated. Binding was detected using antibodies against DDR2 ECD. (b) Inhibition of fibrillogenesis of bovine-dermal collagen I assessed using turbidity measurements. DDR2 ECD proteins (40 μg/ml) as indicated were incubated with 200 μg/ml of neutralized collagen I in 96-well plates at 37 °C.

37 °C), consistent with fibril formation. Under similar conditions, addition of oligomeric DDR2-Fc to the collagen I solution strongly inhibited fibrillogenesis, as determined by the ~80% lower turbidity of the solution at 6 h when compared to collagen alone ($p < 0.0001$). As a control, addition of the anti-Fc antibody to the collagen solution had no significant ($p > 0.9$) effect on collagen turbidity, demonstrating that the effect observed on fibrillogenesis was specific to the DDR2 ECD protein. Dimeric DDR2-Fc also inhibited fibrillogenesis (~60% decrease in turbidity; $p < 0.0001$) albeit less efficiently than the oligomeric DDR2-Fc form ($p < 0.0001$ for DDR2 dimer *versus* oligomer). Monomeric DDR2-V5-His, on the other hand, had no significant effect on collagen fibrillogenesis ($p > 0.1$). Similar experiments were carried out to examine how the oligomeric state of DDR2 ECD modulated fibrillogenesis of rat-tail collagen I. As shown in Fig. S2b, neutralized rat-tail collagen reached maximum turbidity much earlier (within ~1 h) as compared to bovine-dermal collagen. Both oligomeric

and dimeric DDR2-Fc inhibited fibrillogenesis of rat-tail collagen but to a lesser extent (~30% decrease in turbidity; $p < 0.01$) than that observed for bovine-dermal collagen. In addition, no significant differences were observed on the ability of dimeric *versus* oligomeric DDR2 ECD to inhibit fibrillogenesis of rat-tail collagen ($p > 0.2$). Consistent with the results for bovine-dermal collagen (Fig. 2b), monomeric DDR2-V5-His and anti-Fc antibody had no significant effect on the fibrillogenesis of rat-tail collagen ($p > 0.6$). Taken together, these studies demonstrate that increasing the oligomeric state of the DDR2 ECD enhances its binding to collagen I and its ability to inhibit collagen fibrillogenesis.

Oligomeric status of recombinant DDR2 ECD post-ligand binding

Previous studies have demonstrated that collagen I can induce oligomerization of DDR1 ECD [18] as well

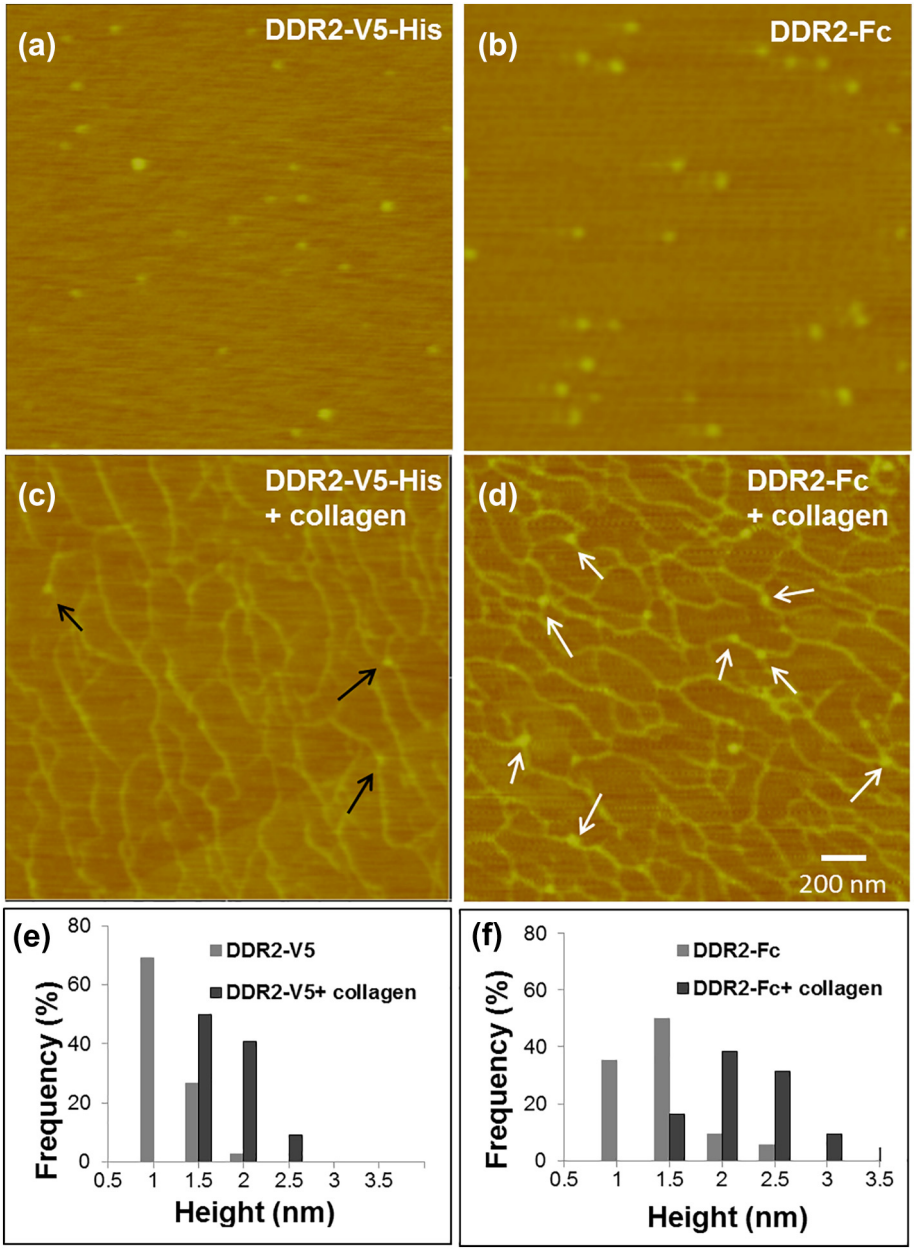

Fig. 3. AFM height images of monomeric DDR2-V5-His and dimeric DDR2-Fc before and after binding to bovine-dermal collagen I as indicated (a–d). DDR2-V5-His and DDR2-Fc particles bound to collagen are indicated by black and white arrows, respectively. Particle size distribution and average sizes are indicated in the accompanying histograms in panels e and f and in Table 1.

as of the full-length [16] and kinase-dead DDR1 [20] receptor. Therefore, we asked whether, under the experimental conditions used here, ligand binding promotes oligomerization and/or clustering of the DDR2 ECD. To this end, we performed single-molecule AFM imaging and analysis of monomeric DDR2-V5-His and dimeric DDR2-Fc before and after binding to collagen [18]. AFM is especially useful to resolve single-molecule interactions and oligomer formation as it can quantify particle sizes with sub-nm resolution and does not require labeling or fixing of biomolecules. AFM imaging has been previously used to study oligomerization of various proteins such as EGF receptors [26], amyloid β protein [27], matrix protein M1 [28], c rings of F-ATP synthases [29], and apoferritin [30], among others.

As shown in the AFM images of Fig. 3, in the absence of collagen I, both DDR2-V5-His and DDR2-Fc imaged as a globular protein with a single lobe. AFM height measurements revealed that DDR2-Fc was ~0.2 nm larger in size ($p < 0.0001$) when compared to DDR2-V5-His (Table 1), consistent with its higher molecular mass detected by SDS-PAGE (Fig. 1b). Upon incubation with collagen I, globular particles binding to collagen filaments could be easily identified in AFM images. It is interesting to note that DDR2-Fc exhibited a higher frequency of binding events when compared to DDR2-V5-His, in agreement with the stronger binding observed in the solid-phase binding assays (Fig. 2a). Quantitative analysis of AFM images revealed that both the monomeric and dimeric proteins exhibited an increase in particle height upon collagen binding when compared to their respective unbound states (Table 1, $p < 0.0001$) when measured with respect to the underlying mica substrate. However, unlike DDR1-Fc, which formed clusters over two-fold in size upon collagen binding [18], the increase in height of DDR2-ECD proteins bound to collagen was only ~1 nm with no changes in the morphology of the bound protein. To determine whether the increase in the protein size in the presence of collagen I represented an additive effect caused by the collagen filaments, we also determined the height of bound DDR2 proteins with respect to collagen filament. As shown in Table 1, both DDR2-V5-His and DDR2-Fc molecules, when measured with respect to their bound collagen filament, displayed a height similar to that of unbound proteins with no significant differences. This indicated that the collagen topography accounted for the increase in height observed for the bound proteins. Thus, the relative size of DDR2 ECD monomers or dimers did not change significantly upon binding to collagen I. Our results thus show that, unlike DDR1-Fc [18], the DDR2 ECD monomers (DDR2-V5-His) or dimers (DDR2-Fc) do not form clusters or higher-order oligomers post-ligand binding.

Clustering and spatial distribution of DDRs in cells post-ligand binding

To examine the effect of collagen on DDR clustering and/or distribution in cells, we used mouse pre-osteoblasts MC3T3-E1 cells as a model system. Morphologically, these cells display extensive cell spreading and a low height profile in tissue culture dishes, two features that make these cells well suited for wide-field fluorescence microscopy and live cell imaging (Fig. 4a–g). MC3T3-E1 cells express readily detectable DDR2 and relatively lower levels of DDR1, under steady-state conditions (Fig. 4h). This profile of expression of DDRs is consistent with these cells being of mesenchymal origin.

To study DDR clustering and spatial distribution in response to collagen stimulation, MC3T3-E1 cells were transiently transfected with vector plasmids encoding full-length human DDR1b-YFP or DDR2-GFP. Receptor clustering and spatial distribution before and after collagen stimulation was examined by fluorescence microscopy at the indicated times. As shown in Fig. 4a and e, before collagen stimulation, both DDR1b-YFP and DDR2-GFP exhibited a uniform distribution of fluorescence on the cells with very few small globular structures, present primarily in the perinuclear region. Control non-transfected cells showed no fluorescent signal (data not shown). When examined at 30 min after administration of bovine-dermal collagen I, DDR1b-YFP displayed a noticeable redistribution revealed by the formation of punctuate structures with a tubular "squiggle" like morphology (henceforth called DDR1b clusters) (Fig. 4b). In a sub-population of cells, these DDR1b clusters persisted even after 4 h of collagen stimulation (Fig. 4c). Quantitative analysis of microscopy images (Fig. S1a) revealed that cells displaying DDR1b clusters were characterized by

Table 1. Topographic height (nm) of DDR2 ECD proteins from AFM images

	Relative to mica		Relative to collagen	*p* Value	
	−Collagen (1)	+Collagen (2)	+Collagen (3)	(1) *versus* (2)	(1) *versus* (3)
DDR2-V5	0.92 ± 0.26 (71)	1.53 ± 0.25 (22)	0.97 ± 0.22 (22)	<0.001*	0.462
DDR2-Fc	1.17 ± 0.40 (74)	2.15 ± 0.49 (50)	1.24 ± 0.48 (50)	<0.001*	0.346

Number in parenthesis indicates total number of particles measured.
* Statistically significant difference.

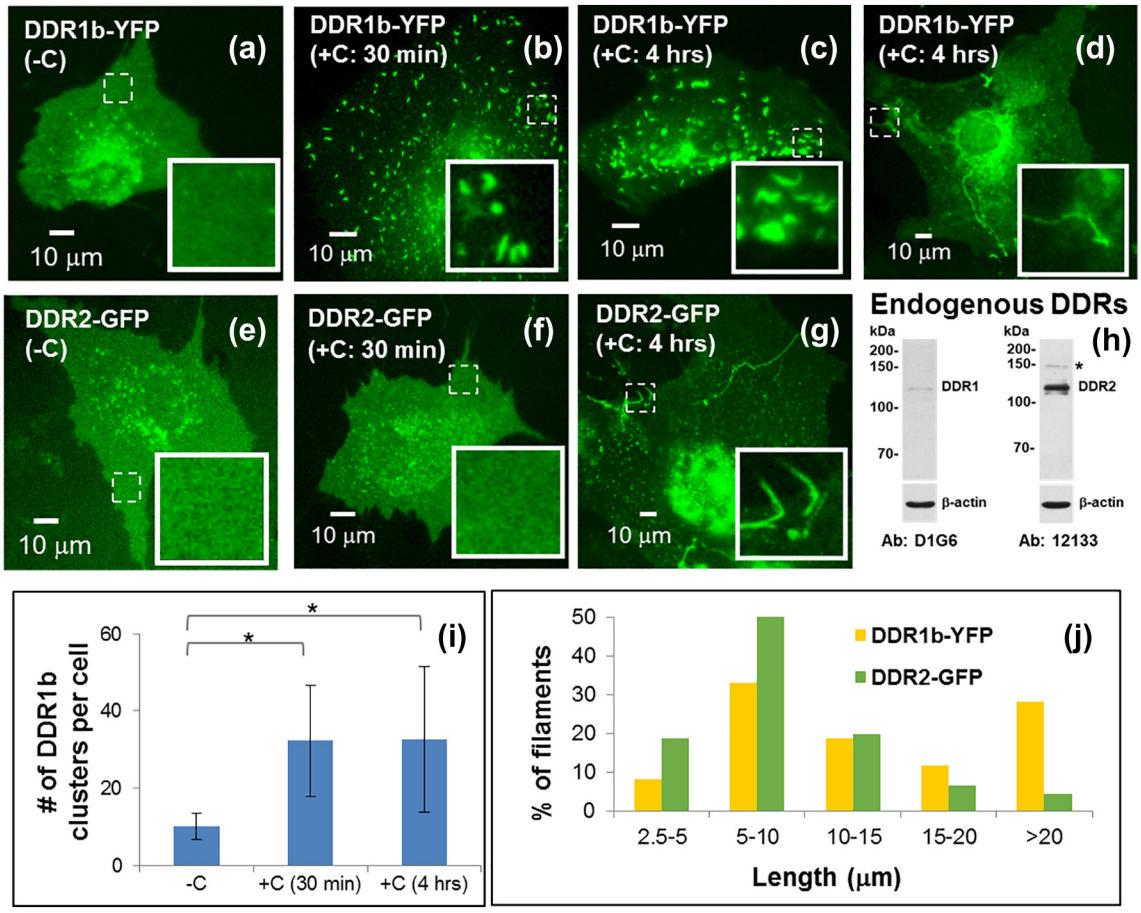

Fig. 4. Live cell imaging of DDR1b-YFP- (a–d) and DDR2-GFP- (e–g) expressing MC3T3-E1 cells using wide-field fluorescence microscopy, before and after the addition of collagen "C" as indicated. Insets (in panels a–g) show selected regions, which have been magnified from the corresponding images to visualize receptor assemblies. The location of these selected regions on the cell surface is indicated by dashed boxes. Endogenous DDR expression in MC3T3-E1 cells was evaluated using Western blotting panel h. Lysates of MC3T3-E1 cells were resolved by reducing 7.5% SDS-PAGE followed by immunoblot analyses using the indicated DDR antibodies. Asterisk (*) shows a non-specific band. Fluorescence microscopy images (a–c) show that DDR1b-YFP exhibits a uniform distribution on the cell surface before collagen stimulation and results in cluster formation upon collagen stimulation. Quantitative analysis (i) indicates that the number of punctuate structures in cells significantly increases upon collagen stimulation ($*p < 0.05$) and persist at 4 h. After 4 h of collagen stimulation, a subpopulation of DDR1b-YFP-expressing cells also exhibits the presence of long, filamentous structures (d). DDR2-GFP exhibits a uniform distribution on the cell surface before collagen stimulation (e) and does not result in cluster formation upon collagen stimulation (f). However, at 4 h post-collagen administration, filamentous structures were also observed in DDR2-GFP-expressing cells (g). The distribution of uninterrupted contour length of filamentous structures formed in DDR1b-YFP- and DDR2-GFP-expressing cells after 4 h of collagen stimulation is shown in panel j.

over 3-fold increase ($p < 0.001$) in the number of punctuate structures when compared to non-stimulated cells (Fig. 4i). These YFP-positive DDR1b clusters persisted at a similar density ($p > 0.05$) even at 4 h post-collagen stimulation in several cells. A similar spatial distribution of DDR1b-YFP was observed when cells were imaged after fixing them at specific time points after collagen stimulation (Fig. S3b).

Interestingly, at prolonged (4 h) stimulation times with collagen I, a sub-population of DDR1b-YFP-expressing cells exhibited the formation of filamentous structures with strong YFP signal, which were different in morphology than the DDR1b clusters (Fig. 4d). Such filamentous structures were found regardless of whether the cells displayed presence of DDR1b clusters (as shown subsequently in Figs. 6a, 9a, and S3). Unlike DDR1b-YFP clusters, which were observed as early as 30 min after collagen administration, the filamentous structures were rarely observed before the 4-h time point (Fig. S3a). Thus, DDR1b-YFP receptors exhibited both cluster formation as well as assembly into filamentous structures, albeit at different time points

after collagen stimulation. DDR2-GFP, in contrast to DDR1b-YFP, showed no obvious signs of receptor redistribution or clustering in response to collagen I at the 30-min time point (Fig. 4f) or even up to 2 h (Fig. S3c). However, at 4 h, a subpopulation of DDR2-GFP-expressing cells demonstrated the presence of GFP-positive filamentous structures, similar to those found in DDR1b-YFP-expressing cells (Figs. 4g and S3c). As was the case for DDR1b-YFP, the filamentous structures formed by DDR2-GFP were rarely observed before the 4-h time point (Fig. S3d). Quantitative analysis of the length of filamentous structures (Fig. S1b) revealed that their maximum un-interrupted contours were several microns in length (Fig. 4j). Interestingly, the average length of filamentous structures analyzed from n = 12 cells was significantly higher ($p < 0.001$) for DDR1b-YFP cells (16.63 ± 12.93 μm) when compared to those present in DDR2-GFP (9.69 ± 6.78 μm) cells. A similar assembly of DDRs into filamentous structures was observed when the cells were stimulated using rat-tail collagen instead of bovine-dermal collagen (Fig. S4). Taken together, these results show that (1) DDR1b and DDR2 differ in their ability to form receptor clusters shortly after

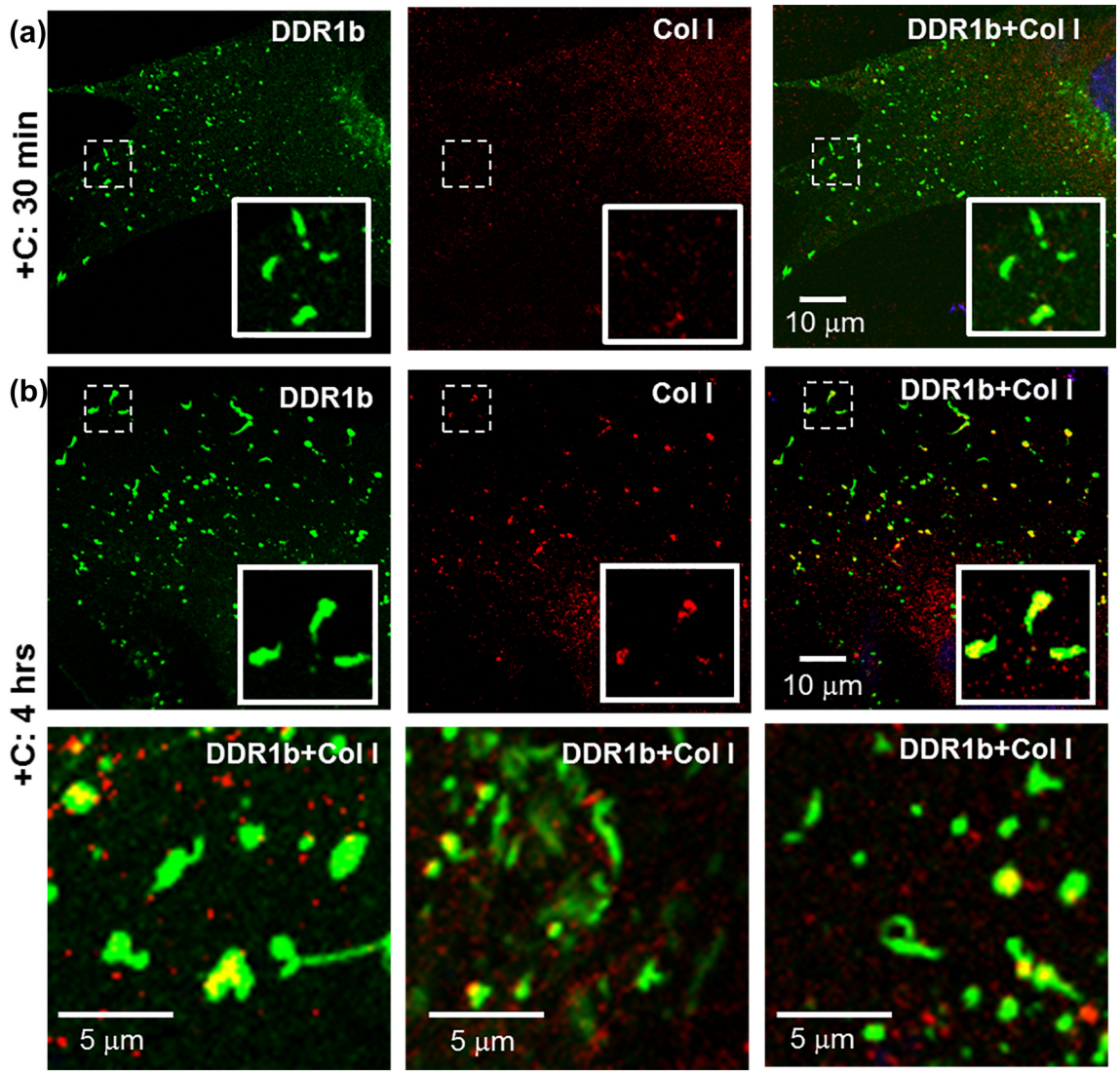

Fig. 5. ICC performed on non-permeabilized cells for evaluating the association of collagen I with DDR1b-YFP clusters. Total receptor is indicated in YFP channel (green), while staining with collagen I antibodies is shown in TRITC channel (red). Co-localization of YFP and TRITC is shown in yellow. Blue represents nuclear (DAPI) staining. Insets (in first row of each panel) show selected regions, which have been magnified form the corresponding images. (a) Little to no signal for collagen staining was detected on cells stimulated with collagen for 30 min, despite the presence of DDR1b clusters. (b) At prolonged collagen stimulation (4 h), a number of DDR1b clusters co-localized with signals for collagen I antibodies. The second row consists of selected regions from three different cells showing co-localization of DDR1b clusters and collagen signal. The collagen associated with DDR1b clusters was non-fibrillar in morphology.

administration of soluble collagen, and (2) both receptors are partly localized in filamentous structures formed upon prolonged collagen stimulation.

Relationship of DDR clusters and filamentous structures with collagen fibrillogenesis

We have shown that DDRs assemble into higher-order structures (clusters or filamentous structures) upon collagen interaction. At the same time, it is well established that collagen I spontaneously undergoes fibrillogenesis and assembles into fibrils. To gain insight into whether collagen fibrillogenesis has an impact on the receptor assembly as described above, we performed ICC. MC3T3 cells expressing YFP/GFP labeled DDRs were stimulated with collagen and subjected to ICC using antibodies against collagen I. These experiments were performed with non-permeabilized cells to specifically follow the fibril formation of the exogenously added collagen on the cell surface. As shown in Fig. 5a, DDR1b clusters, formed in cells stimulated with bovine-dermal collagen for 30 min, showed little to no co-localization with collagen antibody. We surmise that this lack of co-localization may be due to the rapid internalization of DDR1b clusters after collagen stimulation [16]. However, 4 h after collagen stimulation, a sub-population of DDR1b clusters exhibited a partial co-localization ($R = 0.67 \pm 0.19$, Table 2) with collagen (Fig. 5b), suggesting that by this time interval, a fraction of DDR1b clusters may have recycled back to the cell surface. It is interesting to note that the collagen associated with DDR1b clusters displayed a short, non-fibrillar morphology (and not several microns long collagen fibrils), which is characteristic of the early stages of collagen fibrillogenesis.

Next, we examined the relationship between the filamentous structures formed by DDR1b-YFP and DDR2-GFP and the state of collagen fibrillogenesis, using ICC as performed for DDR1b clusters. As shown in Fig. 6, immuno-stained collagen fibrils were detected on the cell surfaces and also found to extend into the peri- and extra-cellular space. The filamentous structures formed by DDR1b-YFP and DDR2-GFP exhibited a morphology that was very similar to that displayed by immuno-stained collagen fibrils, as resolved using our light microscopy-based approaches. Interestingly, staining for collagen was intermittently present and interspersed with the YFP/GFP-positive filamentous structures, indicating that DDR1b-YFP and DDR2-GFP were contiguous with the collagen fibrils. Segments of DDR1b-YFP filamentous structures also exhibited partial co-localization with the collagen fibrils ($R = 0.43 \pm 0.10$, Table 2). In several instances, the filamentous structures formed by both DDR1b-YFP and DDR2-GFP were found to be anchoring collagen fibrils at the cell edges. Taken together, these results suggest that the clusters *versus* filamentous structures formed by DDRs are associated with different morphological states of collagen present at the early *versus* late stage of collagen fibrillogenesis.

Evaluation of DDR phosphorylation and antibody specificity

DDRs undergo receptor phosphorylation upon collagen binding. Therefore, we next aimed to evaluate the spatial distribution of phosphorylated DDR species in MC3T3-E1 cells upon collagen stimulation. To this end, we took advantage of the availability of several antibodies directed against specific phospho-tyrosine residues in collagen-activated DDRs. We employed Western blotting to evaluate the specificity and cross-reactivity of the antibodies against total and phosphorylated receptors in lysates of both MC3T3-E1 and Cos1 cells transiently transfected to express DDR1b-YFP or DDR2-GFP, followed by treatment with or without collagen I. Figure 7a and b shows the profile of total and phosphorylated DDRs in MC3T3-E1 cells before and after collagen stimulation. Without collagen, the D1G6 antibody, an antibody to DDR1 that binds to an epitope within the C-terminal region, detected the full-length recombinant DDR1b-YFP (~140 kDa), as expected, but also detected additional weaker bands at ~120 and

Table 2. Pearson's correlation coefficient (R) for co-localization of YFP/GFP signal with antibody (Ab) signals in ICC samples processed after 4 h of collagen administration

	Ab: Collagen I		Ab: DDR1-Y792		Ab: DDR1b/c-Y513	
	+	−	+	−	+	−
DDR1b-YFP clusters	0.67 ± 0.19**	0.12 ± 0.12	ND	ND	0.86 ± 0.08**	0.22 ± 0.16
DDR1b-YFP filaments	0.43 ± 0.10**	0.12 ± 0.09	0.75 ± 0.10**	0.18 ± 0.08	0.82 ± 0.03**	0.22 ± 0.24

	Ab: Collagen I		Ab: DDR2-Y740			
	+	−	+	−		
DDR2-GFP filaments	ND	ND	0.81 ± 0.06**	0.36 ± 0.13	NA	NA

NA, not applicable; ND, not determined (very few positive correlations found).
** $p < 0.0001$ for YFP/GFP-positive ROIs with (+) *versus* without (−) antibody signal.

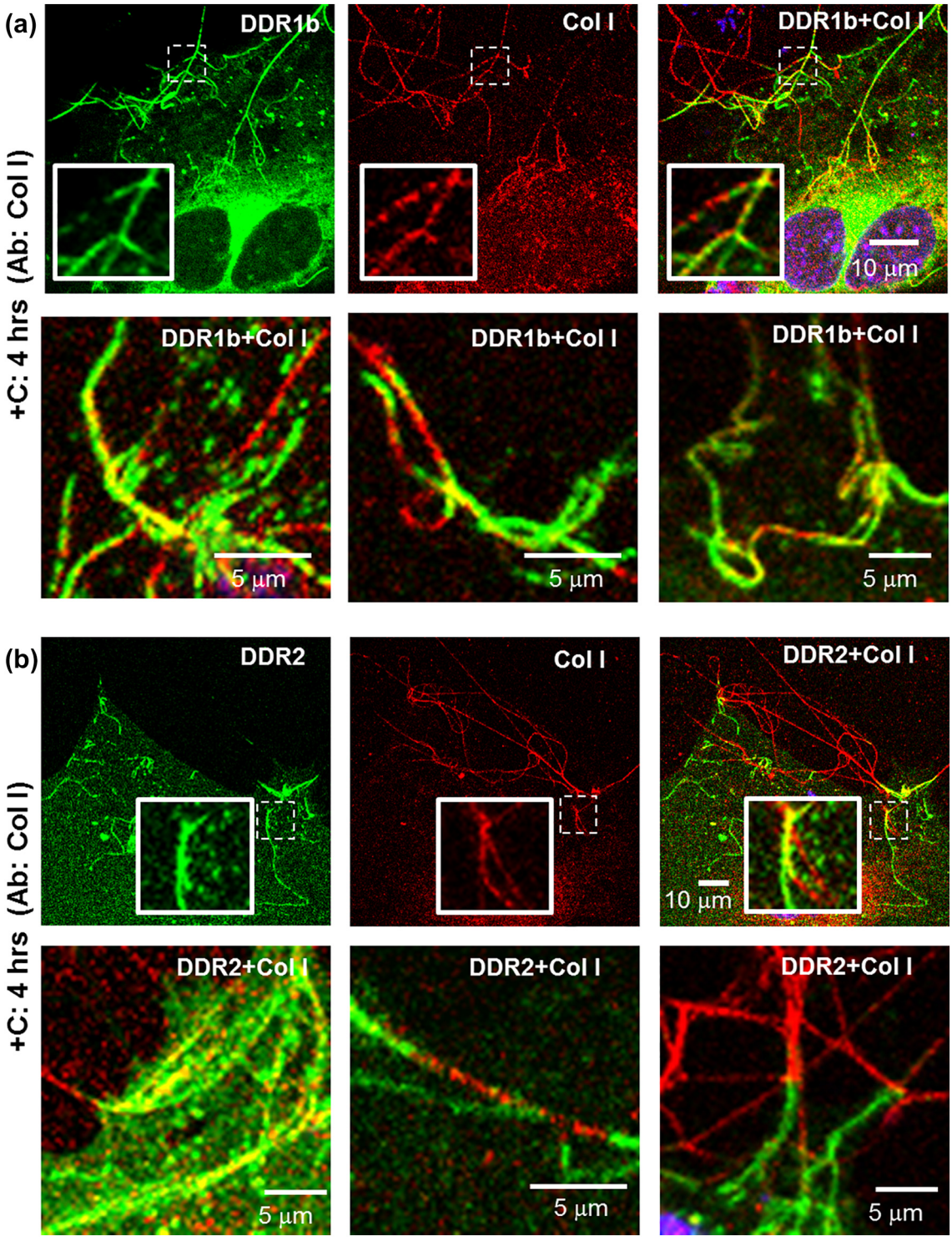

Fig. 6. ICC performed on non-permeabilized cells for evaluating the association of collagen I with filamentous structures formed in (a) DDR1b-YFP- and (b) DDR2-GFP-expressing cells after 4 h of collagen stimulation. Total receptor is indicated in YFP channel (green), while staining with collagen antibodies is shown by TRITC (red). Co-localization YFP and TRITC is shown in yellow. Blue represents nuclear (DAPI) staining. Insets (in first row of each panel) show selected regions, which have been magnified from the corresponding images. Selected regions from three different cells are shown in the second row in each panel. YFP/GFP-positive filamentous structures had a very similar morphology as collagen fibrils and were observed to anchor the fibrils at cell edges. Collagen staining was intermittently present on or interspersed with YFP/GFP-positive filamentous structures.

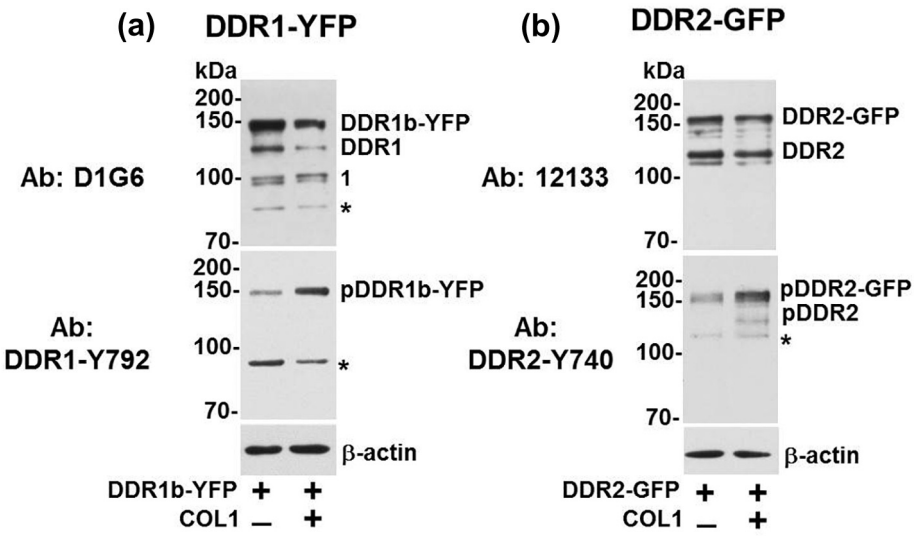

Fig. 7. Western blotting of DDR expression and phosphorylation in MC3T3 cells. MC3T3-E1 cells were transiently transfected with (a) DDR1b-YFP or (b) DDR2-GFP expression vectors and stimulated with 20 μg/ml collagen I (+), as described in Materials and Methods. After 4 h of collagen stimulation, the cells were lysed in RIPA buffer and equal protein concentrations (25 μg/lane) were resolved by reducing 7.5% SDS-PAGE followed by immunoblot analyses using the indicated antibodies to DDR1 or DDR2. β-Actin was used as loading control. Number 1 in panel a indicates an additional band detected with D1G6 antibodies (discussed in the Results section). Asterisks (*) show non-specific bands.

~95–90 kDa (Fig. 7a). The ~120 kDa represents endogenous full-length DDR1 (indicated as DDR1) of MC3T3-E1 cells, whereas the bands of ~95–90 kDa (labeled as #1) are likely to represent proteolytically cleaved DDR1b-YFP receptors lacking the ECD but retaining a membrane-tethered species containing the intracellular juxtamembrane region (IJXM) and the kinase domain (KD) [31]. The D1G6 antibody also reacted with a non-specific band of ~85 kDa (asterisk in D1G6 panel). Upon stimulation with collagen I, total DDR1b-YFP levels decreased, as detected with the D1G6 antibody. However, whether this decrease in total receptor levels is due to variations in transfection efficiency or receptor stability and/or turnover upon collagen stimulation is unclear.

DDR1b-YFP phosphorylation in response to collagen I was evaluated with DDR1-Y792 antibody, which is directed against the phosphorylated Tyr792 residue present within the activation loop of the DDR1 KD. As shown in Fig. 7a (lower panel), this antibody detected phosphorylated DDR1b-YFP (indicated as pDDR1b-YFP) in response to collagen stimulation. However, we also detected basal activation of DDR1b-YFP, likely due to collagen synthesis by these mouse pre-osteoblast cells. Under the same electrophoretic and exposure conditions, phosphorylation of the endogenous DDR1 was undetectable, consistent with the low levels of DDR1 expression in MC3T3-E1 cells (as shown in Fig. 4h). Finally, DDR1-Y792 antibody also displayed cross-reactivity with a non-specific band of ~80-85 kDa (Fig. 7a, lower panel, asterisk).

Lysates of MC3T3-E1 cells transfected with DDR2-GFP-expressing vectors revealed the presence of the recombinant receptor (~160 kDa), as well as the endogenous DDR2 (~120 kDa, indicated as DDR2), as determined with the DDR2 antibody, 12133 (Fig. 7b, upper panel). Exposure to collagen I resulted in phosphorylation of both the endogenous and the recombinant DDR2, as determined with antibody DDR2-Y740, which recognizes a phosphorylated Tyr residue within the activation loop of the DDR2 KD [32] (Fig. 7b, lower panel). The DDR2-Y740 antibody also detected a non-specific band of ~110 kDa. Without exogenous collagen I, we also observed basal levels of DDR2-GFP activation (Fig. 7b), possibly due to collagen synthesis by these cells.

We also evaluated the phospho-DDR (pDDR) antibodies, namely, DDR1-Y792, DDR2-Y740, and the antibody DDR1b/c-Y513, in a time-course experiment of collagen-induced phosphorylation of DDR1b-YFP and DDR2-GFP in transiently transfected Cos1, monkey kidney fibroblast-like cells (Fig. S5). We utilized Cos1 cells because these cells express undetectable endogenous levels of both DDR1 and DDR2 [31] and yield robust expression of recombinant proteins upon transient transfection. The antibody DDR1b/c-Y513 reacts with a phosphorylated Tyr residue at position 513 of the IJXM of DDR1b and DDR1c isoforms [1]. Untransfected or transiently transfected Cos1 cells were stimulated with collagen I for various times. The cell lysates were then examined for DDR phosphorylation using the antibodies to pDDRs. As shown in Fig. S5, both DDR1b-YFP (panel a) and DDR2-GFP (panel b) were activated in response to collagen I, which was evident as early as 30 min after ligand addition, and continued even after 240 min as revealed

with DDR1b/c-Y513, DDR1-Y792, and DDR2-Y740 antibodies, which detected the respective phosphorylated receptor species. We also found that DDR1-Y792 antibodies, as opposed to DDR1b/c-Y513 antibodies, detected a few minor non-specific bands (Fig. S5a, asterisks). D1G6 antibodies readily reacted with full-length (~140 kDa) and (possibly) with a cleaved (~90 kDa) form of DDR1-YFP (indicated by #2). It also showed weak immunoreactivity with a minor non-specific band (Fig. S5a, asterisk). DDR2-Y740 antibody demonstrated strong reactivity with pDDR2-GFP and showed little to no immunoreactivity with other proteins, under these conditions (Fig. S5b). Antibody 12133 against total DDR2 recognized DDR2-GFP, as expected, but also displayed cross-reactivity with a species of ~80 kDa, under these conditions. We also noticed a slight decrease in total DDR2-GFP after collagen stimulation when compared to unstimulated

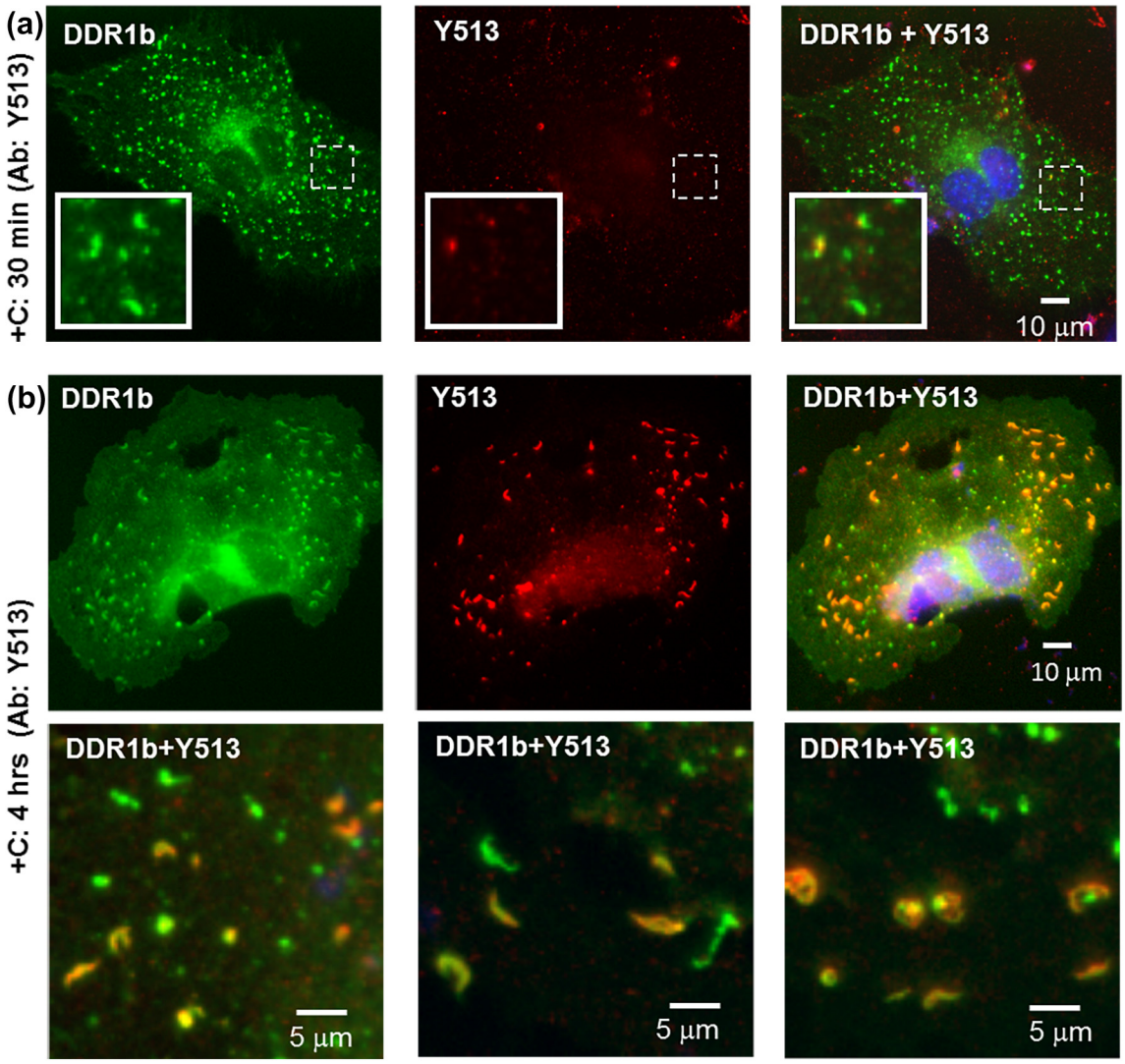

Fig. 8. ICC performed on permeabilized cells for evaluating receptor phosphorylation associated with DDR1b clusters by using pDDR1 antibodies Y513 and Y792, as indicated. Total receptor is indicated in YFP channel (green), while staining with Y513 or Y792 antibodies is shown by TRITC (red). Co-localization YFP and TRITC is shown in yellow. Blue represents nuclear (DAPI) staining. Insets (in first row in panels a and c) show selected regions, which have been magnified from the corresponding images. (a) Little to no Y513 signal was detected in cells, 30 min after collagen stimulation despite the presence of DDR1b clusters. (b) At prolonged collagen stimulation (4 h), a number of DDR1b clusters co-localized with antibodies to Y513. The second row consists of selected regions from three different cells showing co-localization of DDR1b clusters with Y513 signal. (c) Little to no Y792 antibody signal was detected in cells even after 4 h of collagen stimulation despite the presence of DDR1b clusters. The second row consists of selected regions from three different cells showing the presence of DDR1b clusters with little to no co-localization with Y792 signal.

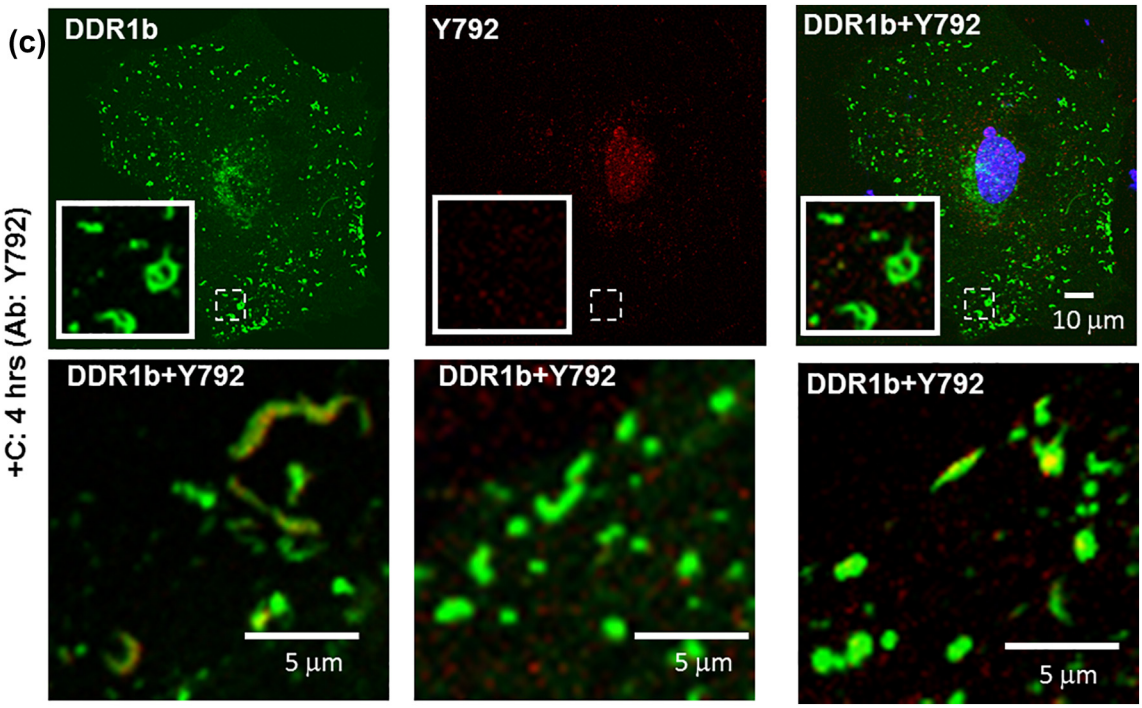

Fig. 8. (*continued*).

cells (Fig. S5b). However, whether this decrease is due the characteristic variability in transient transfection experiments or an inherent effect of collagen-mediated receptor stimulation on DDR2 turnover, remains unclear.

We next evaluated the cross-reactivity of these antibodies against the homologous DDR receptors, namely, whether the pDDR1 antibodies cross-reacted with pDDR2 and vice versa (Fig. S6). We used lysates of untransfected and DDR1b-YFP- or DDR2-GFP-transfected Cos1 cells stimulated with collagen. These analyses showed that the DDR1 antibodies D1G6 and Y513 showed high specificity toward total and phosphorylated DDR1b-YFP, respectively (Fig. S6a, lane 2). DDR1b/c-Y513 antibody also recognized a ~95-kDa species (Fig. S6a), which is likely to represent cleaved phosphorylated DDR1b [31]. Importantly, neither DDR1b/c-Y513 nor D1G6 antibodies showed cross-reactivity against DDR2-GFP (Fig. S6a, lane 3), under the experimental conditions. The DDR1-Y792 recognized pDDR1b-YFP (Fig. S6a), as expected, but also displayed some cross-reactivity against pDDR2-GFP (Fig. S6a, lane 3) and against a non-specific band of ~90 kDa (Fig. S6, lane 3). The 12133 antibodies against total DDR2 strongly reacted with DDR2-GFP (Fig. S6b, lane 6) and showed no cross-reactivity with DDR1b-YFP (Fig. S6b, lane 5). The DDR2-Y740 antibody to pDDR2 recognized pDDR2-GFP but also showed clear immunoreactivity against pDDR1b-YFP (Fig. S6b, lanes 6 and 5 respectively).

Spatial distribution of DDR phosphorylation

After verifying the expression and phosphorylation of DDR1b-YFP and DDR2-GFP in transiently transfected cells and the specificity of the DDR antibodies, we examined the spatial distribution of DDR receptor phosphorylation in MC3T3-E1 cells upon collagen stimulation by using ICC and fluorescence microscopy (Figs. 8–10). As shown in Fig. 8a, a strong signal of YFP-positive clusters was detected at 30 min of administration of bovine-dermal collagen I, as described earlier (Fig. 4b). However, the DDR1b/c-Y513 antibody (Fig. 8a, center panel) and DDR1-Y792 antibody (not shown) displayed little to no co-localization with the DDR1b clusters at the 30-min time point. After 4 h of collagen stimulation, DDR1b/c-Y513 antibody signal exhibited a high degree of co-localization with the YFP-positive clusters with little to no signal present in other regions of the cell ($R = 0.86 \pm 0.08$; Table 2 and Fig. 8b). However, even at 4 h after collagen stimulation, not all DDR1b-YFP clusters showed co-localization with Y513 signal. Interestingly, under the same conditions, little to no signal was observed with the DDR1-Y792 antibody (Fig. 8c). No signal with either DDR1b/c-Y513 or DDR1-Y792 antibodies was detected in untransfected cells regardless of collagen treatment (data not shown). Thus, we surmise that, at 4 h post-ligand administration in DDR1b-YFP-expressing MC3T3-E1 cells, the DDR1b/c-Y513 antibody signals represent DDR1b clusters that are particularly enriched with

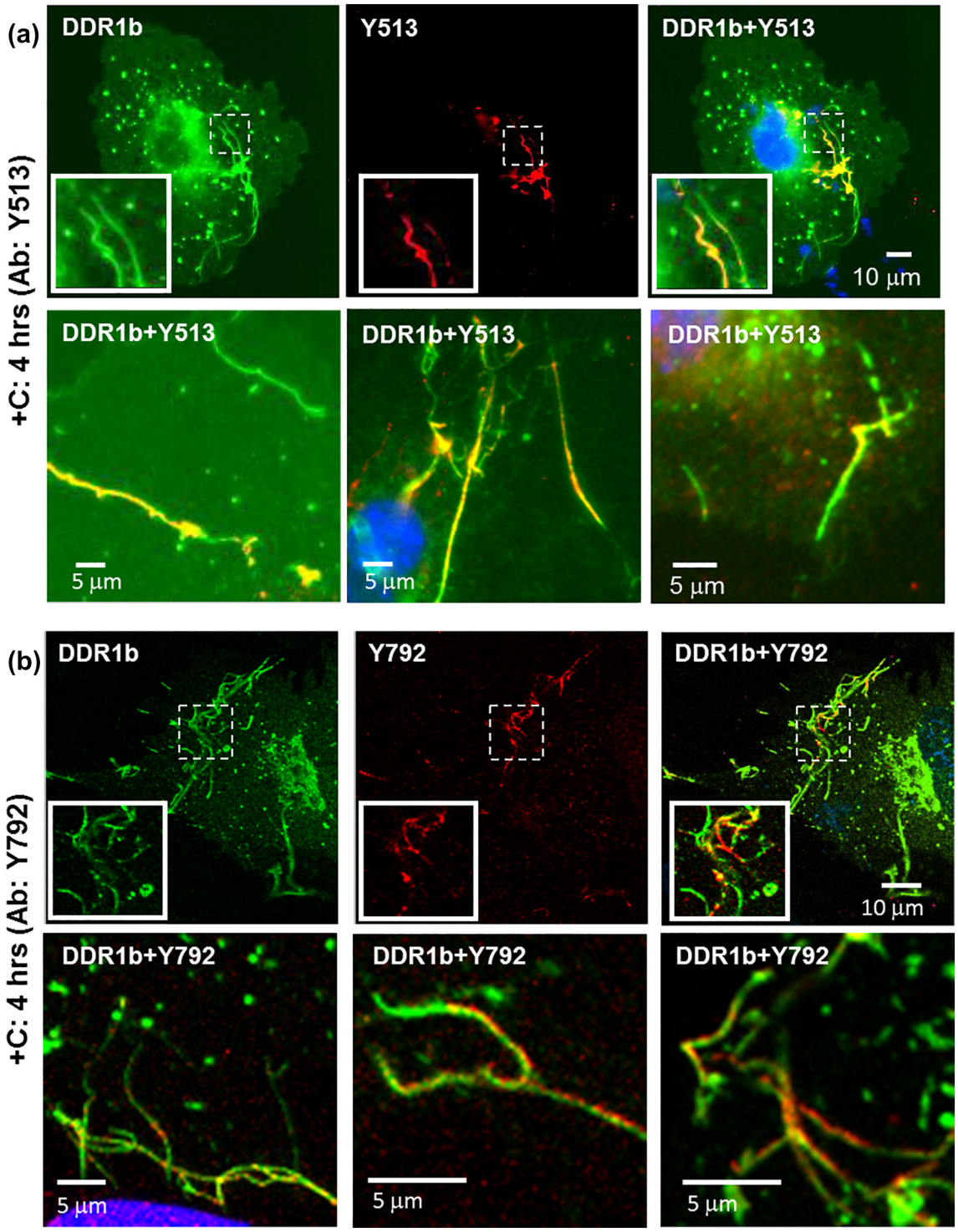

Fig. 9. ICC performed on permeabilized cells for evaluating receptor phosphorylation associated with filamentous structures formed in DDR1b-YFP-expressing cells after 4 h of collagen stimulation, using pDDR1 antibodies (a) Y513 and (b) Y792 as indicated. Total receptor is indicated in YFP channel (green), while staining with Y513 and Y792 antibodies is shown by TRITC (red). Co-localization of YFP and TRITC is shown in yellow. Blue represents nuclear (DAPI) staining. Insets (in first row in each panel) show selected regions, which have been magnified from corresponding images. A subset of DDR1b filamentous structures co-localize with the pDDR1 antibodies. The second row in each panel consists of selected regions from three different cells showing co-localization of filamentous structures with signal for pDDR1 antibodies.

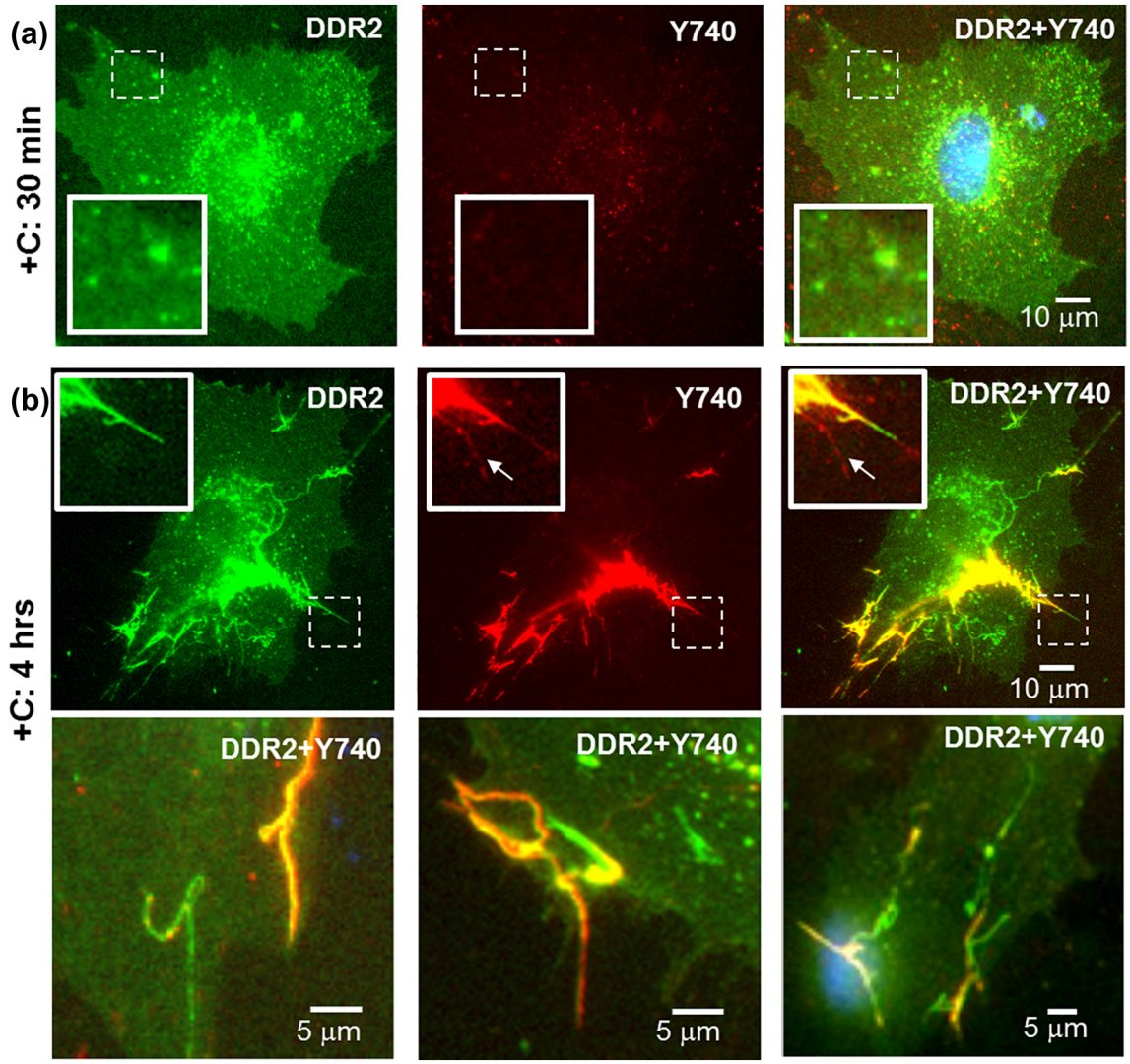

Fig. 10. ICC performed on permeabilized cells for evaluating spatial distribution of receptor phosphorylation in DDR2-GFP-expressing cells after (a) 30 min and (b) 4 h of collagen stimulation. Total receptor is indicated in GFP channel (green), while staining with pDDR2 (Y740) antibodies is shown by TRITC (red). Co-localization GFP and TRITC is shown in yellow. Blue represents nuclear (DAPI) staining. Insets (in top row in each panel) show selected regions, which have been magnified from corresponding images. Little to no co-localization signal was detected, 30 min after collagen stimulation (a). At prolonged collagen stimulation (4 h), a number of filamentous structures formed in DDR2-GFP expressing cells co-localized with Y740 signal (b). The second row in panel b consists of selected regions from three different cells showing co-localization of filamentous structures with Y740 signal. A weak signal for Y740 (arrows) without a corresponding GFP signal can be observed in insets in (b, top row), which could correspond to endogenous pDDR2.

phosphorylated receptor at Y513. While we cannot rule out issues of differential antibody affinities and/or epitope masking, these data suggest the interesting possibility that the two phosphorylation sites of DDR1b, namely, Y513 in the IJXM *versus* Y792 in the KD, are differentially localized in collagen-stimulated MC3T3-E1 cells under these conditions.

We next examined whether the DDR1b/c-Y513 and DDR1-Y792 antibody signals co-localized with the filamentous structures observed in cells after 4 h of collagen I stimulation (Fig. 4d). As shown in Fig. 9, immunostaining with DDR1b/c-Y513 or DDR1-Y792 antibodies revealed co-localization ($R = 0.82 \pm 0.03$ and 0.75 ± 0.10, respectively) of the fluorescent signal with segments of the filamentous structures, suggesting that these structures are sites containing pDDR1b. Of note, DDR1-Y792 antibody (but not DDR1b/c-Y513) signals were also occasionally observed in segments of the filamentous structures, which were devoid of YFP signal. This could be due

to differences in antibody affinities and/or cross-reactivity of DDR1-Y792 antibody with the endogenous phosphorylated DDR2 (Fig. S6a, lane 3).

Analyses of MC3T3-E1 cells expressing DDR2-GFP showed little to no fluorescent signal with DDR2-Y740 antibody at the early (30 min) time point (Fig. 10a). However, after 4 h of collagen simulation, the bulk of DDR2-Y740 signal co-localized ($R = 0.81 \pm 0.06$, Table 2) with the GFP-positive filamentous structures, with minimal signal in other parts of the cell (Fig. 10b). Occasionally, a weak DDR2-Y740 antibody signal was also observed on filamentous structures devoid of GFP signal, which likely represents endogenous pDDR2 (inset in Fig. 10b). Thus, these data suggest that pDDR2 is present within the filamentous structures, as we could not find such significant staining in other locations of DDR2-GFP-expressing cells or in non-transfected cells (data not shown). Interestingly, as observed with the DDR1b-YFP, not all DDR2-GFP-positive filamentous structures co-localized with the DDR2-Y740 antibody signal. A similar pattern of spatial distribution of antibody signals was observed when the cells were stimulated with rat collagen I instead of bovine-dermal collagen (Fig. S7). These findings of YFP and GFP fluorescence co-localizing with ICC signals produced by antibodies recognizing pDDRs in clusters and filamentous structures (as detailed above) suggest that these structures represent sites of receptor phosphorylation in transfected MC3T3-E1 cells.

Discussion

DDRs are type I transmembrane proteins in which their ECD is exposed to the extracellular milieu, ready to interact with collagens. On the plasma membrane, DDRs are displayed as a mixture of monomeric and homodimeric forms, and thus, they also exist as inactive preformed non-covalent homodimers [15]. Here we focused on the specific contribution of isolated ECDs of DDR2, capable of displaying monomeric, dimeric, or oligomeric forms, on collagen binding and collagen fibrillogenesis *in vitro*. We found that oligomeric and dimeric DDR2 ECD species showed the highest affinity toward immobilized collagen I, when compared to the monomeric form. These results are in agreement with earlier reports showing that a dimeric state of DDR2 ECD is required for high-affinity binding to collagen I [7] and oligomeric state of DDR2 ECD enhanced its binding to collagen [22]. Our results also help resolve the discrepancies arising from the different binding assays utilized in these earlier reports. Furthermore, pre-oligomerization of DDR2-Fc enhanced collagen binding in solid-phase binding assays in a manner similar to that observed for DDR1-Fc [18]. Conversely, monomeric DDR2-V5-His exhibited reduced binding, consistent with earlier reports using monomeric His-DS2, which comprised only the DDR2 discoidin domain [7,9]. It is important to note that in an earlier study, amino-terminal tagged His-DDR2 ECD was characterized to be a non-covalently linked dimer [7]. This difference in the oligomeric state of His-tagged DDR2 ECD from this earlier work *versus* our current study could be due to the different sites for epitope tagging and/or differences in protein purification protocols.

One possible explanation for differences in the binding ability of monomeric *versus* dimeric forms of DDR2 ECD to collagen could be that the monomeric form only binds to the primary GVMGFO site, whereas dimeric (and oligomeric) DDR2 ECD binds to additional sites on the collagen triple-helical molecule. Our results from AFM imaging support this hypothesis because the binding events for dimeric DDR2-Fc were observed to be more frequent than those for monomeric DDR2-V5-His on the collagen triple-helical molecule, under identical experimental conditions. Our earlier AFM studies had showed the existence of three possible binding sites for DDR2-Fc oligomers on the collagen I triple helix [11]. Recent studies using col II and col III toolkit peptides have identified that besides the primary GVMGFO site, four additional DDR2 binding sites exist on the collagen triple helix [13,14]. Molecular modeling [13] and X-ray crystallographic studies [8] have provided insight into how the monomeric and dimeric forms of the DDR2 ECD can bind to the GVMGFO site, but no such studies exist for the remaining DDR2 binding sites. Although not discussed by the authors of these studies, it is interesting to note that in their toolkit studies, the various DDR2 ECD variants (including monomeric and dimeric DDR2 ECD) showed different relative affinities to these additional binding sites [13,14]. For instance, while dimeric DDR2-Fc recognized the toolkit peptide II-5 [14], this site was not recognized by DDR2-His [13]. Thus, it is likely that binding of dimeric (and oligomeric) DDR2 ECD to additional sites on the collagen triple-helix could account for their stronger binding and inhibition of collagen fibrillogenesis when compared to the monomeric DDR2 ECD form.

It is interesting to note that our results show a very similar behavior in binding of DDR2 ECD to immobilized a-telo (bovine-dermal) *versus* telo-(rat-tail) collagen I as a function of its oligomeric state. Thus, the telopeptide region of tropocollagen exerts little influence on DDR2-collagen binding, consistent with earlier findings that DDRs bind to the collagen triple-helix [6,33]. However, the presence of telopeptides did influence the modulation of collagen fibrillogenesis by DDR2 ECDs. Oligomeric and dimeric DDR2 ECD inhibited fibrillogenesis of the rat-tail collagen to a much lesser extent as compared to the bovine-dermal collagen. One possible explanation for the reduced effect of DDR2 ECD on fibrillogenesis of telo- collagen could be the differences in the rate of fibrillogenesis *versus* that of

binding of DDR2 ECD to the collagen triple helix. As shown in our studies, the telo- rat-tail collagen exhibited a faster rate of fibrillogenesis and an overall higher turbidity when compared to the a-telo bovine-dermal collagen, consistent with the important role of telopeptides in promoting collagen fibrillogenesis [34]. Our earlier studies using surface plasmon resonance have shown that binding of DDR2-Fc oligomers to immobilized collagen did not reach a saturation even after ~10 min [22]. These observations suggest that the binding of DDR2 ECD to the collagen triple helix may be slow in comparison to the rate of fibrillogenesis of telo-collagen.

A notable feature in our findings was the dissimilarity in the clustering ability of dimeric DDR1 ECD (DDR1-Fc) *versus* that of DDR2-Fc post-ligand binding, which was evident in the results from our AFM experiments. While the recombinant DDR1-Fc ECD spontaneously clustered to form high-order structures upon collagen binding *in vitro* [18], no such feature was observed for DDR2-Fc. Measurement of particle sizes from AFM images revealed that DDR2-Fc preserved its globular morphology and size post-collagen binding. Consistent with these *in vitro* observations, live-cell imaging showed that while the full-length DDR1b-YFP underwent a spatial re-distribution and cluster formation within minutes after collagen stimulation [16], DDR2-GFP maintained a homogenous distribution on the cell surface with no clustering at similar time points. While we cannot completely rule out potential contributions of the TMD or ICD domains of DDR2 in small cluster formation, which could not be resolved by wide-field light microscopy of cells, our results suggest that, unlike DDR1b, DDR2 is not able to organize into large clusters upon ligand binding. Interestingly, while clustering of DDR1b-YFP was observed in the MC3T3-E1 cells utilized in this study, clustering of DDR1 upon collagen stimulation has also been reported in other cell types, for example, HEK293 [16], Cos-7 [21], and GD25 [20], by us and others, suggesting that DDR1 clustering is likely a ubiquitous phenomenon.

Our results suggest that formation of DDR1b clusters may be important for and precede receptor phosphorylation. Indeed, while DDR1b clustering was readily detected (by YFP signal) 30 min after collagen administration, phosphorylated DDR1 species at Y513 (present in the IJXM) were evident after 4 h of collagen stimulation. Furthermore, the observation that not all DDR1b clusters were positive for Y513 signal lends support to the hypothesis that receptor clustering may be a prerequisite for receptor phosphorylation. Moreover, our findings that DDR1b clusters were positive for Y513 and not Y792 (present in the KD) suggest that differentially phosphorylated DDR1b receptor subpopulations may be segregated to various subcellular sites. However, whether the stronger detection of DDR1b/c-Y513 *versus* DDR1-Y792 signals in DDR1b clusters is due to differences in antibody affinity or differences in epitope availability and/or phosphorylation/dephosphorylation kinetics needs to be determined.

Despite the differences in the clustering abilities of DDR1b *versus* DDR2 upon ligand administration, we also noted striking similarities in the spatial distribution and phosphorylation of DDR1b-YFP and DDR2-GFP. We show for the first time that in MC3T3-E1 cells, after 4 h of collagen administration, both DDR1b-YFP and DDR2-GFP assemble into filamentous structures. A fraction of these filamentous structures was positively highlighted by DDR1b/c-Y513, DDR1-Y792, and DDR2-Y740 antibodies. Our observations that not all filamentous structures were positive for these antibodies suggest that, like DDR1b clustering, the assembly of DDRs into filamentous structures may precede receptor phosphorylation.

Recent studies have reported the co-localization of total and pDDRs in cells with collagen [20,21,35]. Our results expand these observations by showing that higher-order assembly of DDRs into receptor clusters and/or filamentous structures may associate with different morphological states of collagen. While the DDR1b clusters (formed at early time points after collagen stimulation) associated with non-fibrillar collagen, the DDR1b/DDR2 filamentous structures (formed after prolonged collagen stimulation) associated with collagen fibrils. It should be noted that in this study soluble collagen was presented to the cells, which could spontaneously assemble into fibrils and/or undergo a cell-mediated assembly into fibrils. These processes could dictate if the formation of collagen fibrils is a prerequisite for, is synchronous with, or succeeds the assembly of DDRs into filamentous structures in cells. Our observations that the filamentous structures formed by DDRs do not evolve with time but only appear after prolonged collagen stimulation and are contiguous with collagen fibrils even in the peri-cellular regions suggest that a fibrillar form of collagen may be required to assemble DDRs. Further studies using multi-modal high-resolution microscopy to monitor DDRs as well as collagen morphology on the cell surface at various time points or presenting the cells with preformed collagen fibrils instead of soluble collagen will be required to understand the role of collagen fibrillogenesis and the fibrillar state of collagen in clustering, spatio-temporal distribution, and phosphorylation of DDRs. Our current study using soluble collagen I holds relevance primarily for extracellular matrix remodeling when newly synthesized soluble collagen is presented to the cells. Further studies are needed to fully comprehend the role of DDRs in health and disease by investigating how DDRs bind and respond to fibrils of collagen I as well as to other collagen types present in natural tissues.

Besides collagen, other cytoskeletal and/or intracellular proteins could also have a putative role in modulating the spatial distribution and assembly of DDRs into clusters or filamentous structures. Our initial

investigations to identify such proteins yielded limited success. Both DDR1b clusters as well as DDR1b and DDR2 filamentous structures did not co-localize with either vimentin, vinculin (Fig. S8), or f-actin (Fig. S9). This is consistent with an earlier report showing the lack of co-localization between DDR1 with these cytoskeletal proteins in cells cultured on immobilized collagen fibrils [20]. However, DDR1 has been reported to co-localize with non-muscle myosin II [20]. Along similar lines, we found that the filamentous structures formed by DDR1b-YFP and DDR2-GFP were enriched with the actin-binding protein cortactin (Fig. S10). It is tempting to speculate that the higher-order assembly of DDRs into filamentous structures may serve as a scaffold for recruiting proteins like cortactin and myosin II to communicate with the cell cytoskeleton. In this regard, it is important to note that DDRs have reported to play a role in cell-mediated traction forces and mechano-transduction [20] and in formation of linear invadosomes [36]. Further studies are required to understand how the DDR–collagen assembly and ensuing receptor phosphorylation may be involved in these processes.

Collectively, the results presented here provide new insights into ligand binding, clustering, spatial distribution, and phosphorylation of DDR1b and DDR2 in response to soluble collagen I. As depicted in the cartoon of Scheme 1, we postulate a model in which the spatial distribution and assembly of DDRs is dependent on the morphological state of collagen and precedes receptor phosphorylation. In this model, we propose that DDR1b cluster formation is promoted by the presence of non-fibrillar collagen present during the early stages of collagen fibrillogenesis. These DDR1b clusters undergo endocytosis to early endosomes, within a few minutes of collagen stimulation, as

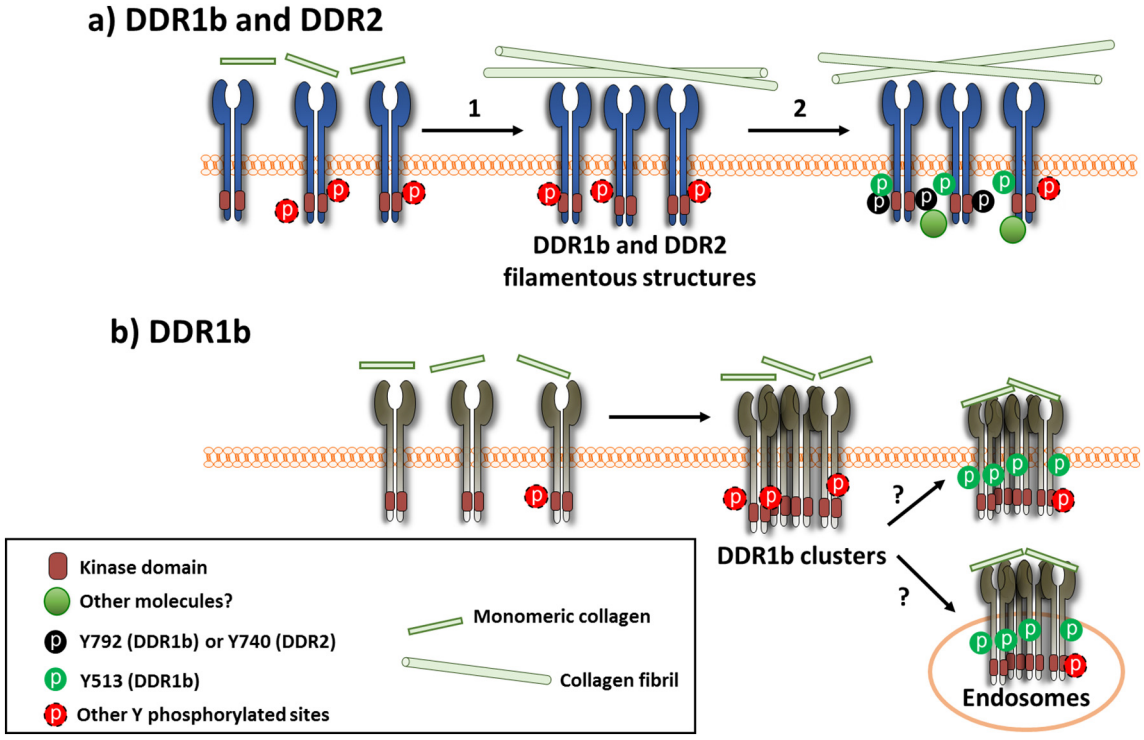

Scheme 1. Postulated model for spatial distribution and phosphorylation of DDRs upon collagen stimulation. DDR1 and DDR2 exist as homodimers on the cell surface. (a) Upon addition of monomeric collagen I, DDR1 and DDR2 interact with collagen, which leads (arrow 1) to the assembly of the receptors into filamentous structures aligned with collagen fibrils. This process occurs at prolonged (~4 h) times after collagen I stimulation. Phosphorylation of both DDR1 and DDR2 (arrow 2) co-localizes in these structures, as determined using Y513 (pDDR1b) as well as Y792 (pDDR1) and Y740 (pDDR2) antibodies, indicated as black and green circles. (b) In another pathway, DDR1b assembles into clusters within minutes of collagen I stimulation (likely binding to non-fibrillar collagen present at early stages of fibrillogenesis) and gets endocytosed. However, phosphorylation at Y513 and Y792 is not detected in these clusters at the early (~30 min) time point. At later times (~4 h) post-ligand administration, phosphorylation of DDR1b in its IJXM (Y513) (green circles) but not in its KD (Y792) is detected in the DDR1b clusters. At present, it is not clear if Y513-positive clusters are present on the cell surface or constitute pools of endocytosed DDR1b receptors localizing within endosomes. Owing to the fact that DDRs contain numerous Tyr residues within the IJXM region and their KDs, phosphorylation at other Tyr residues (indicated by the red dashed circles) may also be ensuing in the structures described in panels a and b but are undetectable by the tools available at this time. It is likely that formation of higher-order assemblies of DDRs may recruit additional cytosolic proteins, which mediate specific cellular processes.

shown in our earlier studies [16]. At later time points, a fraction of DDR1b receptor clusters may recycle back to the plasma membrane with their cargo. During this process of recycling, a sub-population of DDR1b clusters is enriched with phosphorylated receptor species at Y513. Whether these phosphorylated DDR1b clusters localize in the endosome or the cell-membrane cannot be presently deciphered. Further studies are required to dissect the molecular composition and sub-cellular location of DDR1b clusters, which may be responsible for specific cell-signaling pathways, as has been defined for other members of the receptor tyrosine kinase family [37,38]. In this regard, it is interesting to note that DDR1 has also been reported to co-internalize with and phosphorylate upon stimulation of insulin-like-growth factor I (IGF-IR) receptor, and the collagen-dependent phosphorylation of DDR1 was impaired in the absence of IGF-IR [39].

The close physical association of collagen fibrils with DDR1b-YFP and DDR2-GFP filamentous structures suggests that the formation of collagen fibrils, upon addition of exogenous monomeric collagen, may be important for the assembly of DDRs into filamentous structures. The assembly of DDRs into filamentous structures may be a prerequisite for receptor phosphorylation. The time required for collagen fibril formation may in part explain the delayed kinetics of DDR phosphorylation in response to soluble collagen. We propose that the clusters and filamentous structures of DDR1b (and likely DDR1c) are characterized by different phosphorylation sites: (i) DDR1b clusters are enriched with Y513 phosphorylation and (ii) DDR1b filamentous structures are enriched with tyrosine phosphorylation at both the IJXM (Y513) and KD (Y792). In the case of DDR2, phosphorylation within the KD (at Y740) appears to be spatially confined to filamentous structures. Thus, DDR1b and DDR2 may share common (filamentous structures) and distinct (clusters) spatial sites and supramolecular states, and phosphorylation profiles in response to collagen stimulation. Regardless, our studies highlight the complexities of factors involved in DDR receptor phosphorylation and the corresponding distribution of the ligand and receptor assemblies within the cellular environment.

Finally, it is important to emphasize the limitations and sensitivity of the techniques and reagents used (e.g., a limited number of anti-phosphotyrosine antibodies) here to follow the spatial–temporal profile of receptor phosphorylation. Another caveat in our studies was that only partial and/or intermittent co-localization of immuno-stained collagen was observed with the clusters and filamentous structures formed by DDRs. We postulate that this could be due to masking of antibody-recognizing epitopes on collagen as a result of DDR binding. Future studies using additional antibodies, fluorescently labeled collagen, submicroscopic high-resolution imaging of molecular complexes, laser capture-microdissection [40] and identification of phosphorylated receptor species by phospho-proteomics approaches at various time points are warranted to elucidate the state of collagen and of these unique collagen receptors upon ligand interactions.

Acknowledgment

This work was supported by NSF CMMI award 1201111 to G.A., AHA predoctoral award 16PRE31160013 to D.Y., and grants from the NIH-NCI (CA1986), Department of Defense (W81XWH-15-1-0226), and the Sky Foundation to R.F. We acknowledge Nabanita Chatterjee at OSU for her assistance with cell-culture experiments.

Appendix A. Supplementary data

Supplementary data to this article can be found online at https://doi.org/10.1016/j.jmb.2018.11.015.

Received 5 March 2018;
Received in revised form 6 November 2018;
Accepted 14 November 2018
Available online 17 November 2018

Keywords:
atomic force microscopy;
fibrillogenesis;
fluorescence microscopy;
oligomer;
receptor tyrosine kinase

Abbreviations used:
AFM, atomic force microscopy; DDR1, discoidin domain receptor 1; DDR2, discoidin domain receptor 2; ECD, extracellular domain; GFP, green fluorescent protein; ICC, immunocytochemistry; ICD, intracellular domain; IJXM, intracellular juxtamembrane region; KD, Kinase Domain; PBS, phosphate-buffered saline; pDDR, phosphorylated discoidin domain receptor; TMD, transmembrane domain; YFP, yellow fluorescent protein.

References

[1] H.-L. Fu, R.R. Valiathan, R. Arkwright, A. Sohail, C. Mihai, M. Kumarasiri, K.V. Mahasenan, S. Mobashery, P. Huang, G. Agarwal, R. Fridman, Discoidin domain receptors: unique receptor tyrosine kinases in collagen-mediated signaling, J. Biol. Chem. 288 (2013), https://doi.org/10.1074/jbc.R112.444158.

[2] L.A. Flynn, A.R. Blissett, E.P. Calomeni, G. Agarwal, Inhibition of collagen fibrillogenesis by cells expressing

soluble extracellular domains of DDR1 and DDR2, J. Mol. Biol. 395 (2010), https://doi.org/10.1016/j.jmb.2009.10.073.
[3] G. Agarwal, DDRs and collagen fibrillogenesis, Discoidin Domain Recept. Heal. Dis 2016, pp. 23–56.
[4] J.R. Tonniges, B. Albert, E.P. Calomeni, S. Roy, J. Lee, X. Mo, S.E. Cole, G. Agarwal, Collagen fibril ultrastructure in mice lacking discoidin domain receptor 1, Microsc. Microanal. 22 (2016) 599–611, https://doi.org/10.1017/S1431927616000787.
[5] B. Leitinger, Discoidin domain receptor functions in physiological and pathological conditions, Int. Rev. Cell Mol. Biol. 310 (2014) 39–87, https://doi.org/10.1016/B978-0-12-800180-6.00002-5.
[6] W. Vogel, G.D. Gish, F. Alves, T. Pawson, The discoidin domain receptor tyrosine kinases are activated by collagen, Mol. Cell 1 (1997) 13–23, https://doi.org/10.1016/S1097-2765(00)80003-9.
[7] B. Leitinger, Molecular analysis of collagen binding by the human discoidin domain receptors, DDR1 and DDR2. Identification of collagen binding sites in DDR2, J. Biol. Chem. 278 (2003) 16761–16769, https://doi.org/10.1074/jbc.M301370200.
[8] F. Carafoli, D. Bihan, S. Stathopoulos, A.D. Konitsiotis, M. Kvansakul, R.W. Farndale, B. Leitinger, E. Hohenester, Crystallographic insight into collagen recognition by discoidin domain receptor 2, Structure 17 (2009) 1573–1581, https://doi.org/10.1016/j.str.2009.10.012.
[9] O. Ichikawa, M. Osawa, N. Nishida, N. Goshima, N. Nomura, I. Shimada, Structural basis of the collagen-binding mode of discoidin domain receptor 2, EMBO J. 26 (2007) 4168–4176, https://doi.org/10.1038/sj.emboj.7601833.
[10] F. Carafoli, M.C. Mayer, K. Shiraishi, M.A. Pecheva, L.Y. Chan, R. Nan, B. Leitinger, E. Hohenester, Structure of the discoidin domain receptor 1 extracellular region bound to an inhibitory Fab fragment reveals features important for signaling, Structure 20 (2012) 688–697, https://doi.org/10.1016/j.str.2012.02.011.
[11] G. Agarwal, L. Kovac, C. Radziejewski, S.J. Samuelsson, Binding of discoidin domain receptor 2 to collagen I: an atomic force microscopy investigation, Biochemistry 41 (2002) 11091–11098, https://doi.org/10.1021/bi020087w.
[12] G. Agarwal, C. Mihai, D.F. Iscru, Interaction of discoidin domain receptor 1 with collagen type 1, J. Mol. Biol. 367 (2007) 443–455, https://doi.org/10.1016/j.jmb.2006.12.073.
[13] A.D. Konitsiotis, N. Raynal, D. Bihan, E. Hohenester, R.W. Farndale, B. Leitinger, Characterization of high affinity binding motifs for the discoidin domain receptor DDR2 in collagen, J. Biol. Chem. 283 (2008) 6861–6868, https://doi.org/10.1074/jbc.M709290200.
[14] H. Xu, N. Raynal, S. Stathopoulos, J. Myllyharju, R.W. Farndale, B. Leitinger, Collagen binding specificity of the discoidin domain receptors: binding sites on collagens II and III and molecular determinants for collagen IV recognition by DDR1, Matrix Biol. 30 (2011) 16–26, https://doi.org/10.1016/j.matbio.2010.10.004.
[15] N.A. Noordeen, F. Carafoli, E. Hohenester, M.A. Horton, B. Leitinger, A transmembrane leucine zipper is required for activation of the dimeric receptor tyrosine kinase DDR1, J. Biol. Chem. 281 (2006) 22744–22751, https://doi.org/10.1074/jbc.M603233200.
[16] C. Mihai, M. Chotani, T.S. Elton, G. Agarwal, Mapping of DDR1 distribution and oligomerization on the cell surface by FRET microscopy, J. Mol. Biol. 385 (2009) 432–445.
[17] H.-L. Fu, R.R. Valiathan, L. Payne, M. Kumarasiri, K.V. Mahasenan, S. Mobashery, P. Huang, R. Fridman, Glycosylation at Asn211 regulates the activation state of the discoidin domain receptor 1 (DDR1), J. Biol. Chem. 289 (2014) 9275–9287, https://doi.org/10.1074/jbc.M113.541102.
[18] D. Yeung, D. Chmielewski, C. Mihai, G. Agarwal, Oligomerization of DDR1 ECD affects receptor-ligand binding, J. Struct. Biol. 183 (2013) 495–500, https://doi.org/10.1016/j.jsb.2013.06.010.
[19] H. Xu, T. Abe, J.K.H. Liu, I. Zalivina, E. Hohenester, B. Leitinger, Normal activation of discoidin domain receptor 1 mutants with disulfide cross-links, insertions, or deletions in the extracellular juxtamembrane region: mechanistic implications, J. Biol. Chem. 289 (2014) 13565–13574, https://doi.org/10.1074/jbc.M113.536144.
[20] N. Coelho, P. Arora, S. van Putten, S. Boo, S. Petrovic, A. Lin, B. Hinz, C. McCulloch, Discoidin domain receptor 1 mediates myosin-dependent collagen contraction, Cell Rep. 18 (2017) 1774–1790.
[21] V. Juskaite, D.S. Corcoran, B. Leitinger, Collagen induces activation of DDR1 through lateral dimer association and phosphorylation between dimers, elife 6 (2017), https://doi.org/10.7554/eLife.25716.
[22] C. Mihai, D.F. Iscru, L.J. Druhan, T.S. Elton, G. Agarwal, Discoidin domain receptor 2 inhibits fibrillogenesis of collagen type 1, J. Mol. Biol. 361 (2006) 864–876, https://doi.org/10.1016/j.jmb.2006.06.067.
[23] C. Finger, C. Escher, D. Schneider, The single transmembrane domains of human receptor tyrosine kinases encode self-interactions, Sci. Signal. 2 (2009) ra56, https://doi.org/10.1126/scisignal.2000547.
[24] D. Kim, P. Ko, E. You, S. Rhee, The intracellular juxtamembrane domain of discoidin domain receptor 2 (DDR2) is essential for receptor activation and DDR2-mediated cancer progression, Int. J. Cancer 135 (2014) 2547–2557, https://doi.org/10.1002/ijc.28901.
[25] L. Sivakumar, G. Agarwal, The influence of discoidin domain receptor 2 on the persistence length of collagen type I fibers, Biomaterials 31 (2010) 4802–4808, https://doi.org/10.1016/j.biomaterials.2010.02.070.
[26] C.L. Jia, Z.J. Zhou, R.C. Liu, S.D. Chen, R.H. Xia, EGF receptor clustering is induced by a 0.4 mT power frequency magnetic field and blocked by the EGF receptor tyrosine kinase inhibitor PD153035, Bioelectromagnetics 28 (2007) 197–207, https://doi.org/10.1002/bem.20293.
[27] A. Sebollela, G.M. Mustata, K. Luo, P.T. Velasco, K.L. Viola, E.N. Cline, G.S. Shekhawat, K.C. Wilcox, V.P. Dravid, W.L. Klein, Elucidating molecular mass and shape of a neurotoxic Aβ Oligomer, ACS Chem. Neurosci. 5 (2014) 1238–1245, https://doi.org/10.1021/cn500156r.
[28] M. Hilsch, B. Goldenbogen, C. Sieben, C.T. Höfer, J.P. Rabe, E. Klipp, A. Herrmann, S. Chiantia, Influenza a matrix protein m1 multimerizes upon binding to lipid membranes, Biophys. J. 107 (2014) 912–923, https://doi.org/10.1016/j.bpj.2014.06.042.
[29] D. Pogoryelov, C. Reichen, A.L. Klyszejko, R. Brunisholz, D.J. Muller, P. Dimroth, T. Meier, The oligomeric state of c rings from cyanobacterial F-ATP synthases varies from 13 to 15, J. Bacteriol. 189 (2007) 5895–5902, https://doi.org/10.1128/JB.00581-07.
[30] D.N. Petsev, B.R. Thomas, S.-T. Yau, P.G. Vekilov, Interactions and aggregation of apoferritin molecules in solution: effects of added electrolytes, Biophys. J. 78 (2000) 2060–2069, https://doi.org/10.1016/S0006-3495(00)76753-1.

[31] H.-L. Fu, A. Sohail, R.R. Valiathan, B.D. Wasinski, M. Kumarasiri, K.V. Mahasenan, M.M. Bernardo, D. Tokmina-Roszyk, G.B. Fields, S. Mobashery, R. Fridman, Shedding of discoidin domain receptor 1 by membrane-type matrix metalloproteinases, J. Biol. Chem. 288 (2013) 12114–12129, https://doi.org/10.1074/jbc.M112.409599.

[32] K. Yang, J.H. Kim, H.J. Kim, I.S. Park, I.Y. Kim, B.S. Yang, Tyrosine 740 phosphorylation of discoidin domain receptor 2 by Src stimulates intramolecular autophosphorylation and Shc signaling complex formation, J. Biol. Chem. 280 (2005) 39058–39066, https://doi.org/10.1074/jbc.M506921200.

[33] A. Shrivastava, C. Radziejewski, E. Campbell, L. Kovac, M. McGlynn, T.E. Ryan, S. Davis, M.P. Goldfarb, D.J. Glass, G. Lemke, G.D. Yancopoulos, An orphan receptor tyrosine kinase family whose members serve as nonintegrin collagen receptors, Mol. Cell 1 (1997) 25–34, https://doi.org/10.1016/S1097-2765(00)80004-0.

[34] M. Shayegan, T. Altindal, E. Kiefl, N.R. Forde, Intact telopeptides enhance interactions between collagens, Biophys. J. 111 (2016) 2404–2416, https://doi.org/10.1016/j.bpj.2016.10.039.

[35] M.T. Luczynski, P.T. Harrison, N. Lima, L. Krasny, A. Paul, P.H. Huang, Spatial localisation of discoidin domain receptor 2 (DDR2) signalling is dependent on its collagen binding and kinase activity, Biochem. Biophys. Res. Commun. 501 (2018) 124–130, https://doi.org/10.1016/j.bbrc.2018.04.191.

[36] A. Juin, C. Billottet, V. Moreau, O. Destaing, C. Albiges-Rizo, J. Rosenbaum, E. Génot, F. Saltel, Physiological type I collagen organization induces the formation of a novel class of linear invadosomes, Mol. Biol. Cell 23 (2012) 297–309, https://doi.org/10.1091/mbc.E11-07-0594.

[37] X. Li, A.G. Garrity, H. Xu, Regulation of membrane trafficking by signalling on endosomal and lysosomal membranes, J. Physiol. 591 (2013) 4389–4401, https://doi.org/10.1113/jphysiol.2013.258301.

[38] T. Stasyk, L.A. Huber, Spatio-temporal parameters of endosomal signaling in cancer: implications for new treatment options; spatio-temporal parameters of endosomal signaling in cancer: implications for new treatment options, J. Cell. Biochem. 117 (2016) 836–843, https://doi.org/10.1002/jcb.25418.

[39] R. Malaguarnera, M.L. Nicolosi, A. Sacco, A. Morcavallo, V. Vella, C. Voci, M. Spatuzza, S.-Q. Xu, R.V. Iozzo, R. Vigneri, A. Morrione, A. Belfiore, Novel cross talk between IGF-IR and DDR1 regulates IGF-IR trafficking, signaling and biological responses, Oncotarget 6 (2015), https://doi.org/10.18632/oncotarget.3177.

[40] Z. Ezzoukhry, E. Henriet, F.P. Cordelières, J.W. Dupuy, M. Maître, N. Gay, S. Di-Tommaso, L. Mercier, J.G. Goetz, M. Peter, F. Bard, V. Moreau, A.A. Raymond, F. Saltel, Combining laser capture microdissection and proteomics reveals an active translation machinery controlling invadosome formation, Nat. Commun. 9 (2018), https://doi.org/10.1038/s41467-018-04461-9.